

# Journal Pre-proof

Synthesis, characterization and anion recognition studies of new fluorescent alkyl bis(naphthylureylbenzamide)-based receptors

Luis Miguel Lopéz-Martínez, José García-Elías, Adrián Ochoa-Terán, Hisila Santacruz Ortega, Karen Ochoa-Lara, César Ulises Montaña-Medina, Anatoli K. Yatsimirsky, José Z. Ramírez, Victoria Labastida-Galván, Mario Ordoñez

PII: S0040-4020(19)31222-0

DOI: <https://doi.org/10.1016/j.tet.2019.130815>

Reference: TET 130815

To appear in: *Tetrahedron*

Received Date: 17 October 2019

Revised Date: 15 November 2019

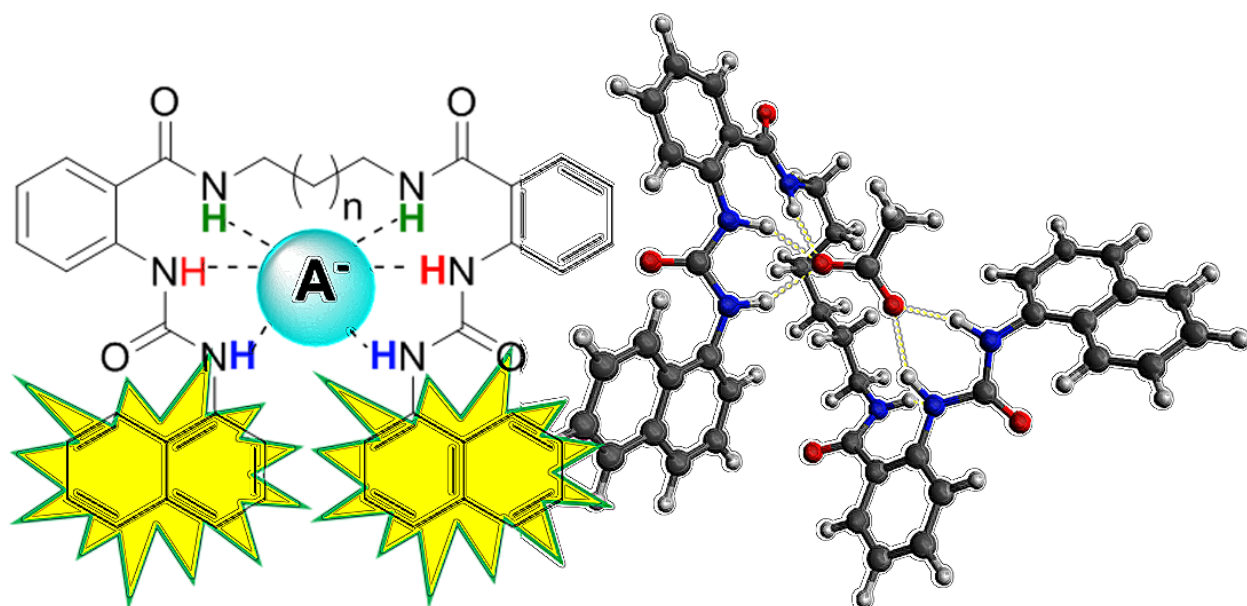
Accepted Date: 19 November 2019

Please cite this article as: Lopéz-Martínez LM, García-Elías José, Ochoa-Terán Adriá, Ortega HS, Ochoa-Lara K, Montaña-Medina CéUlises, Yatsimirsky AK, Ramírez JoséZ, Labastida-Galván V, Ordoñez M, Synthesis, characterization and anion recognition studies of new fluorescent alkyl bis(naphthylureylbenzamide)-based receptors, *Tetrahedron* (2019), doi: <https://doi.org/10.1016/j.tet.2019.130815>.

This is a PDF file of an article that has undergone enhancements after acceptance, such as the addition of a cover page and metadata, and formatting for readability, but it is not yet the definitive version of record. This version will undergo additional copyediting, typesetting and review before it is published in its final form, but we are providing this version to give early visibility of the article. Please note that, during the production process, errors may be discovered which could affect the content, and all legal disclaimers that apply to the journal pertain.

© 2019 Published by Elsevier Ltd.





## Synthesis, characterization and anion recognition studies of new fluorescent alkyl bis(naphthylureylbenzamide)-based receptors

Luis Miguel López-Martínez<sup>1,2</sup>, José García-Elías<sup>3</sup>, Adrián Ochoa-Terán<sup>\*1</sup>, Hisila Santacruz Ortega<sup>4</sup>, Karen Ochoa-Lara<sup>\*4</sup>, César Ulises Montaña-Medina<sup>1</sup>, Anatoli K. Yatsimirsky<sup>5</sup>, José Z. Ramírez,<sup>1</sup> Victoria Labastida-Galván<sup>6</sup> and Mario Ordoñez<sup>6</sup>

<sup>1</sup> Centro de Graduados e Investigación en Química, Tecnológico Nacional de México/IT de Tijuana, Tijuana, B.C. México.

<sup>2</sup> Universidad Estatal de Sonora (UES), Hermosillo, Sonora, México.

<sup>3</sup> Unidad Académica de Ciencias de la Tierra, Universidad Autónoma de Zacatecas, Zacatecas, México.

<sup>4</sup> Departamento de Investigación en Polímeros y Materiales. Universidad de Sonora. Hermosillo, Sonora. México

<sup>5</sup> Facultad de Química, Universidad Nacional Autónoma de México. Ciudad de México. México.

<sup>6</sup> Centro de Investigaciones Químicas-(IICBA), Universidad Autónoma del Estado de Morelos, Cuernavaca, México.

\* Correspondence e-mail: ochoa@tectijuana.mx, karenol@polimeros.uson.mx

### Abstract

The synthesis of new alkyl (C<sub>3</sub> to C<sub>8</sub>) bis(naphthylureylbenzamide)-based receptors and the study of their interaction with anions by UV-Vis, molecular fluorescence and <sup>1</sup>H NMR were performed. The results suggest both ureylbenzamide units participate in the complexation with anions due to their inherent flexibility, which promotes a cooperative binding effect. The position of the urea and amide groups, as well as, the alkyl chain length, have an important influence in the fluorescent response; *meta* receptors present an *ON*<sup>1</sup>/*OFF*/*ON*<sup>2</sup> response, while *ortho* receptors have an *OFF*/*ON* response. The most significant changes were observed with dihydrogen phosphate and hydrogen pyrophosphate due to high affinity for these anions. The <sup>1</sup>H NMR studies show

differences in the interaction sites depending the relative position of the urea and amide groups, as well as, the anion type. Finally, a theoretical analysis of complexes by DFT support the experimental results.

**Keywords:** Anion recognition; fluorescent receptors; bis-urea; benzamide

## Introduction

The selective recognition of anions has been studied over the last two decades and is subject of important research in the supramolecular chemistry field focused to selective recognition of anions with biological importance.<sup>1,2</sup> Anions play an important role in a range of biological processes.<sup>3, 4</sup> They are essential in the formation of a variety of enzyme-substrate and enzyme-cofactor complexes, as well as, in the interaction between proteins and nucleic acids.<sup>5,6</sup> On the other hand, the poor regulation of anion transport mechanisms results in serious complications and diseases, such as cystic fibrosis.<sup>7</sup> Consequently, it is important to develop receptors or sensors that can detect the presence of various anionic species and regulate their transport in biological systems.<sup>8</sup> One way in which host molecules can recognize anionic guests is based on electrostatic interactions.<sup>9</sup> However, host molecules that operate based on this principle often suffer lack of selectivity due to the non-directional properties of electrostatic interactions.<sup>5</sup>

The chromogenic and fluorogenic receptors that include urea groups as a binding subunit have proved to be particularly excellent candidates for recognition of anions, such as fluoride, acetate, dihydrogen phosphate, among others.<sup>3,10,11</sup> A very important motif for anion recognition is the hydrogen bonding because of its directionality, which is extremely useful in design of selective hosts for anions with different geometries.<sup>12,13</sup>

Most of the receptors belonging to this class of urea derivatives are neutral and contain a subunit capable to donate H-bonds to the anion, therefore, anion recognition occurs through the H-bonding interaction of urea N-H hydrogens, to give a stable anion-receptor complex.<sup>1,4,9</sup> The negative charge of anion stabilizes the excited state of the chromophore reducing the energy of urea-to-chromophore charge-transfer transition.<sup>14, 15</sup> On the other hand, deprotonation of one N-H fragment is accompanied by a drastic electron rearrangement in the receptor, which results in a significant change of absorption spectrum, as well as, the pattern of <sup>1</sup>H NMR signals, which makes the process unambiguously discernible.<sup>2,9,14</sup> Also, some receptors that contain thiourea groups as hydrogen bond donors offers a greater opportunity for anion recognition than

urea, due to an enhanced acidity of the N-H bonds, that readily deprotonates with a number of anionic species.<sup>1,11,12,16</sup> These findings demonstrate considerable selectivity for specific anions, even in protic media.<sup>10</sup> The urea (or thiourea) moiety has been used as a host attached to *o*-phenylene,<sup>7,17</sup> *m*-phenylene, *p*-phenylene,<sup>6,11</sup> naphthalene,<sup>18</sup> anthracene, pyrene<sup>19,20</sup> and anthraquinone.<sup>5,21</sup> However, anion selective systems able to operate in aqueous media remains as considerable challenge.<sup>10</sup>

The synthesis of urea-based receptors capable of interact selectively with anions is an important subdiscipline in supramolecular chemistry. The anionic recognition by this type of receptors is mainly based on hydrogen bond donation and the functionality and directionality provided by the N-H group.<sup>22</sup> These characteristics play an important role in selective recognition of anions with different geometries. An example was reported by Amendola *et al.*, where selective binding of urea with acetate was described as a "Y" type arrangement, through two hydrogen bonds provided by the urea in the receptor giving rise to the anionic recognition. In addition, the selectivity is also related to the energy of receptor-anion interaction.<sup>23,24</sup> The strongest interactions of hydrogen bonds are established with the most basic anions such as fluoride, carboxylates and inorganic oxoanions. According to a recent point of view, all hydrogen bonds are considered as proton transfer reactions.<sup>25-27</sup> Therefore, for a receptor containing acid N-H groups, the selectivity is related mainly with the anion basicity or pKa for the conjugate acid. The greater basicity of the anion generates a stronger hydrogen bonding interaction.<sup>28</sup>

Moreover, Dos Santos *et al.* reported receptors with urea and acetamide groups in a different relative position (*ortho*, *meta* and *para*). This investigation showed that the position affects selectivity and stoichiometry of the complexes.<sup>29</sup> In receptors with *meta* and *para* relative position, the anionic recognition is carried out only through the urea group, while the amide group participates only when there is an allosteric change and the conformation is favored to establish a hydrogen bond with the anion, forming a complex with 1:2 stoichiometry. In addition, the receptor with a relative *ortho* position forms complexes with 1:1 stoichiometry, and there is cooperativity from the amide in the complexes.<sup>29</sup>

The bis(urea) receptors have become good hosts for the recognition of anions with different size and geometry, this is attribute to the donation of hydrogens by the N-H groups present in the receptor. However, these receptors also fulfil other important characteristics to increase the viability of molecular recognition as the high structural



## Experimental

### *Materials and equipment*

All reagents and solvents were obtained from commercial suppliers and used without further purification. NMR spectra (400 MHz for  $^1\text{H}$ , 100 MHz for  $^{13}\text{C}$ ) were recorded on a Bruker Avance 400 spectrometer in  $\text{DMSO-}d_6$  at a probe temperature of 23 °C, with TMS as internal standard. Electronic impact mass spectra were obtained by direct insertion in an Agilent 5975C mass spectrometer, and the intensities were reported as a relative percentage to the base peak after the corresponding  $m/z$  value. FAB mass spectra and HRMS were recorded in MStation JMS-700 JOEL. UV-Vis absorption spectra were obtained using a Cary 100 conc UV-Visible spectrophotometer. Fluorescence emission spectra were obtained using a Cary Eclipse fluorescence spectrophotometer.

### *Anion recognition study by UV-Vis titrations*

The effect of anions upon the absorbance was examined adding 6  $\mu\text{L}$  of a  $1 \times 10^{-3}$  M TBAX solution to a known volume (3 mL) of a  $1 \times 10^{-5}$  M receptor solution. The receptors and TBAX stock solutions were prepared in spectroscopic grade acetonitrile. A quartz cuvette was filled with 3 mL of the receptor stock solution, then 6  $\mu\text{L}$  aliquots of TBAX stock solution were added successively with a calibrated micropipette, thus the ratio of the total concentration  $[\text{TBAX}]_t/[\text{L}]_t$  was in a desired range. The resulting complex solutions were stirred for 3 min and the spectra were recorded. The absorption spectrum was confirmed to be unchanged with time at each measurement.

### *Anion recognition study by fluorometric titrations*

The effect of anions upon the emission was examined adding 7.5  $\mu\text{L}$  of a  $1 \times 10^{-3}$  M TBAX solution to a known volume (3 mL) of a  $1 \times 10^{-5}$  M receptor solution. A quartz cuvette was filled with 3 mL of the receptor stock solution, and then 7.5  $\mu\text{L}$  aliquots of TBAX stock solution were added successively with a calibrated micropipette, thus the ratios of the total concentration  $[\text{TBAX}]_t/[\text{L}]_t$  was in a desired range. The resulting complex solutions were stirred for 3 min and the spectra were recorded. The emission intensity was confirmed to be unchanged with time at each measurement.

**Anion recognition study by NMR titrations**

The effect of anions upon the chemical shifts of the receptor signals was examined adding 2  $\mu\text{L}$  of a 0.3 M TBAX stock solution to a known volume (0.5 mL) of a  $6 \times 10^{-3}$  M receptor solution contained in a NMR tube. The addition was limited to 0.056 mL, then the dilution effect was insignificant. For the studies of anion recognition, a  $6 \times 10^{-3}$  M receptor solution was prepared in  $\text{DMSO-}d_6$ , and then 2  $\mu\text{L}$  aliquots of a 0.3 M TBAX stock solution was added with a calibrated micropipette, thus the  $[\text{TBAX}]/[\text{L}]$  ratio was in a desired range. The kinetic study by  $^1\text{H}$  NMR of anion recognition at relationship 1:5 was obtained at temperatures of 277 K.

**Molecular modelling**

The molecular optimization of the receptors and complexes geometries were performed by DFT, the PBE0 functional and the DZVP base were use in Gaussian 09 computational program.<sup>32</sup>

**Synthesis***Synthesis of alkyl bis(2-aminobenzamide) compounds*

In a single neck round bottom flask, the isatoic anhydride (2.9 g, 18.3 mmol) was suspended in 100 mL of dry tetrahydrofuran (THF) with stirring under Ar atmosphere. Then, a condenser was connected to the reaction flask and 8.3 mmol of alkyl diamine (3, 4, 6 and 8 carbons) were added to the mixture. The reaction was refluxed and stirred for 24 h. Then, the solvent was removed by heating under reduced pressure and the product was washed and filtered as many times as needed to give an analytically pure solid compound.

*N,N'*-(propane-1,3-diyl)bis(2-aminobenzamide) (**o3**). White solid. Yield: 40.8%. M. p. 158-160 °C. FT-IR: 3470, 3355, 3294, 3055, 2967, 2931, 1625, 1576, 1531  $\text{cm}^{-1}$ .  $^1\text{H}$  NMR ( $\text{DMSO-}d_6$ , 400 MHz):  $\delta$  8.21 (s, 2 H), 7.47 (d,  $J = 7.7$  Hz, 2 H), 7.13 (t,  $J = 7.2$  Hz, 2 H), 6.69 (d,  $J = 7.7$  Hz, 2 H), 6.51 (t,  $J = 7.2$  Hz, 2 H), 6.37 (s, 4 H), 3.27 (brs, 4 H), 1.81 - 1.61 (m, 2 H).  $^{13}\text{C}$  NMR ( $\text{DMSO-}d_6$ , 100 MHz):  $\delta$  168.8, 149.4, 131.4, 127.8, 116.2, 114.8, 114.5, 36.5, 29.2. MS (FAB<sup>+</sup>): 313  $[\text{M}+\text{H}]^+$ . HRMS (FAB<sup>+</sup>): Calculated for  $\text{C}_{17}\text{H}_{21}\text{N}_4\text{O}_2$ : 313.1665; Found: 313.1599.

*N,N'*-(butane-1,4-diyl)bis(2-aminobenzamide) (**o4**). White solid. Yield: 72.2%. M. p. 190-192 °C. FT-IR: 3469, 3557, 3284, 3056, 2930, 2860, 1621, 1578, 1534  $\text{cm}^{-1}$ .  $^1\text{H}$

NMR (DMSO-*d*<sub>6</sub>, 400 MHz):  $\delta$  8.19 (t, *J* = 4.9 Hz, 2 H), 7.46 (d, *J* = 7.85 Hz, 2 H), 7.12 (t, *J* = 7.4 Hz, 2 H), 6.68 (d, *J* = 7.85 Hz, 2 H), 6.49 (t, *J* = 7.4 Hz, 2 H), 6.36 (brs, 4 H), 3.40 - 3.18 (m, 4 H), 1.59 - 1.49 (m, 4 H). <sup>13</sup>C NMR (DMSO-*d*<sub>6</sub>, 100 MHz):  $\delta$  168.7, 149.4, 131.3, 127.9, 116.2, 114.9, 114.4, 38.4, 26.7. MS (FAB<sup>+</sup>): 326 [M+H]<sup>+</sup>. HRMS (FAB<sup>+</sup>): Calculated for C<sub>18</sub>H<sub>23</sub>N<sub>4</sub>O<sub>2</sub>: 327.1821; Found: 327.1820.

*N,N'*-(hexane-1,6-diyl)bis(2-aminobenzamide) (**o6**). White solid. Yield: 54.8%. M. p. 158-160 °C. FT-IR: 3473, 3668, 3292, 3057, 2926, 2858, 1622, 1581, 1538 cm<sup>-1</sup>. <sup>1</sup>H NMR (DMSO-*d*<sub>6</sub>, 400 MHz):  $\delta$  8.16 (t, *J* = 4.4 Hz, 2 H), 7.45 (d, *J* = 7.9 Hz, 2 H), 7.11 (t, *J* = 7.4 Hz, 2 H), 6.67 (d, *J* = 7.9 Hz, 2 H), 6.50 (t, *J* = 7.4 Hz, 2 H), 6.34 (brs, 4 H), 3.28 - 3.10 (m, 4 H), 1.59 - 1.41 (m, 4 H), 1.41 - 1.22 (m, 4 H). <sup>13</sup>C NMR (DMSO-*d*<sub>6</sub>, 100 MHz):  $\delta$  169.2, 150.0, 131.9, 128.5, 116.7, 115.6, 115.0, 39.2, 29.7, 26.8. MS (FAB<sup>+</sup>): 355 [M+H]<sup>+</sup>. HRMS (FAB<sup>+</sup>): Calculated for C<sub>20</sub>H<sub>27</sub>N<sub>4</sub>O<sub>2</sub>: 355.2134; Found: 355.2120.

*N,N'*-(octane-1,8-diyl)bis(2-aminobenzamide) (**o8**). White solid. Yield: 36.1%. M. p. 164-166 °C. FT-IR: 3475, 3670, 3292, 3057, 2926, 2858, 1622, 1581, 1538 cm<sup>-1</sup>. <sup>1</sup>H NMR (DMSO-*d*<sub>6</sub>, 400 MHz):  $\delta$  8.15 (t, *J* = 4.9 Hz, 2 H), 7.45 (d, *J* = 7.9 Hz, 2 H), 7.11 (t, *J* = 7.4 Hz, 2 H), 6.67 (d, *J* = 7.9 Hz, 2 H), 6.49 (t, *J* = 7.4 Hz, 2 H), 6.35 (brs, 4 H), 3.19 (q, *J* = 6.6 Hz, 4 H), 1.56 - 1.41 (m, 4 H), 1.36 - 1.19 (m, 8 H). <sup>13</sup>C NMR (DMSO-*d*<sub>6</sub>, 100 MHz):  $\delta$  169.2, 150.0, 131.9, 128.5, 116.7, 115.6, 115.0, 39.3, 29.6, 29.3, 27.0. MS (FAB<sup>+</sup>): 383 [M+H]<sup>+</sup>. HRMS (FAB<sup>+</sup>): Calculated for C<sub>22</sub>H<sub>31</sub>N<sub>4</sub>O<sub>2</sub>: 383.2447; Found: 383.2469.

#### *Synthesis of N,N'-alkyl bis(2-(3-(naphthalen-1-yl)ureyl)benzamide) compounds*

In a single neck round bottom flask, 1.0 equivalent of alkyl bis(2-aminobenzamide) (**o3**, **o4**, **o6** or **o8**) was dissolved in 100 mL of dry THF with stirring under Ar atmosphere (15 min). Then, a condenser was connected to the reaction flask and 2.2 equivalent of 1-naphthyl isocyanate was added to the mixture. The reaction was refluxed and stirred for 24 h. Then, the solvent was removed by heating under reduced pressure and the product was washed and filtered as many times as needed to give an analytically pure solid compound.

*N,N'*-(propane-1,3-diyl)bis(2-(3-(naphthalen-1-yl)ureyl)benzamide) (**o3N**). Pearl solid. Yield: 80.3%. M. p. 218-220 °C. FT-IR: 3298, 3051, 3079, 2827, 2852, 1646, 1543 cm<sup>-1</sup>

<sup>1</sup>. <sup>1</sup>H NMR (DMSO-*d*<sub>6</sub>, 400 MHz): δ 10.16 (s, 2 H), 9.58 (s, 2 H), 8.74 (t, *J* = 5.5 Hz, 2 H), 8.23 (d, *J* = 8.3 Hz, 2 H), 8.10 (d, *J* = 8.3 Hz, 2 H), 7.90 (d, *J* = 7.8 Hz, 2 H), 7.75 (d, *J* = 7.3 Hz, 2 H), 7.67 (d, *J* = 8.0 Hz, 2 H), 7.62 (dd, *J* = 7.8, 1.3 Hz, 2 H), 7.53 - 7.38 (m, 8 H), 7.06 (t, *J* = 7.3 Hz, 2 H), 3.45 - 3.37 (m, 4 H), 1.90 - 1.79 (m, 2 H). <sup>13</sup>C NMR (DMSO-*d*<sub>6</sub>, 100 MHz): δ 168.3, 153.3, 139.3, 134.2, 133.7, 131.0, 128.0, 127.7, 127.4, 125.7, 125.4, 123.9, 122.3, 121.0, 120.7, 120.2, 36.7, 28.7. MS (FAB<sup>+</sup>): 651 [M+H]<sup>+</sup>. HRMS (FAB<sup>+</sup>): Calculated for C<sub>39</sub>H<sub>35</sub>N<sub>6</sub>O<sub>4</sub>: 651.2720; Found: 651.2710.

*N,N'*-(butane-1,4-diyl)bis(2-(3-(naphthalen-1-yl)ureyl)benzamide) (**o4N**). Pearl solid. Yield: 58.7%. M. p. 242-244 °C. FT-IR: 3296, 3254, 3069, 2933, 2861, 1735, 1646, 1606, 1543 cm<sup>-1</sup>. <sup>1</sup>H NMR (DMSO-*d*<sub>6</sub>, 400 MHz): δ 10.28 (s, 2 H), 9.62 (s, 2 H), 8.69 (t, *J* = 5.4 Hz, 2 H), 8.19 (d, *J* = 8.3 Hz, 2 H), 8.15 (s, 2 H), 7.92 (s, 2 H), 7.77 - 7.67 (m, 4 H), 7.62 (dd, *J* = 7.8, 1.3 Hz, 2 H), 7.58 - 7.35 (m, 8 H), 7.02 (t, *J* = 7.4 Hz, 2 H), 3.35 - 3.27 (m, 4 H), 1.70 - 1.52 (m, 4 H). <sup>13</sup>C NMR (DMSO-*d*<sub>6</sub>, 100 MHz): δ 168.1, 153.5, 139.5, 134.3, 133.8, 131.0, 128.1, 127.7, 125.8, 125.6, 125.5, 124.1, 122.6, 122.2, 121.0, 120.5, 28.9, 26.3. MS (FAB<sup>+</sup>): 665 [M+H]<sup>+</sup>. HRMS (FAB<sup>+</sup>): Calculated for C<sub>40</sub>H<sub>37</sub>N<sub>6</sub>O<sub>4</sub>: 665.2876; Found: 665.3036.

*N,N'*-(hexane-1,6-diyl)bis(2-(3-(naphthalen-1-yl)ureyl)benzamide) (**o6N**). Pearl solid. Yield: 35.1%. M. p. 220-222 °C. FT-IR: 3298, 3250, 3073, 2930, 2862, 1737, 1645, 1606 cm<sup>-1</sup>. <sup>1</sup>H NMR (DMSO-*d*<sub>6</sub>, 400 MHz): δ 10.24 (s, 2 H), 9.61 (s, 2 H), 8.64 (t, *J* = 4.8 Hz, 1 H), 8.18 (d, *J* = 8.3 Hz, 2 H), 8.14 (d, *J* = 8.8 Hz, 2 H), 7.91 (m, 2 H), 7.72 (d, *J* = 7.3 Hz, 2 H), 7.69 (d, *J* = 8.0 Hz, 2 H), 7.59 (d, *J* = 7.0 Hz, 2 H), 7.56 - 7.36 (m, 8 H), 7.03 (t, *J* = 7.5 Hz, 1 H), 3.27 (q, *J* = 6.3 Hz, 4 H), 1.65 - 1.45 (m, 4 H), 1.44 - 1.25 (m, 4 H). <sup>13</sup>C NMR (DMSO-*d*<sub>6</sub>, 100 MHz): δ 168.9, 154.2, 140.2, 135.0, 134.5, 131.7, 128.8, 128.4, 128.4, 126.5, 126.2, 124.8, 123.3, 122.7, 121.7, 121.3, 41.1, 40.9, 27.2. MS (FAB<sup>+</sup>): 693 [M+H]<sup>+</sup>. HRMS (FAB<sup>+</sup>): Calculated for C<sub>42</sub>H<sub>41</sub>N<sub>6</sub>O<sub>4</sub>: 693.3189; Found: 693.3144.

*N,N'*-(octane-1,8-diyl)bis(2-(3-(naphthalen-1-yl)ureyl)benzamide) (**o8N**). Pearl solid. Yield: 64.4%. M. p. 216-218 °C. FT-IR: 3332, 3269, 3053, 2922, 1693, 1622, 1614, 1603, 1596, 1526 cm<sup>-1</sup>. <sup>1</sup>H NMR (DMSO-*d*<sub>6</sub>, 400 MHz): δ 10.23 (s, 2 H), 9.61 (s, 2 H), 8.62 (t, *J* = 5.3 Hz, 1 H), 8.20 - 8.12 (m, 4 H), 7.95 - 7.89 (m, 2 H), 7.73 (d, *J* = 7.5 Hz, 2 H), 7.69 (d, *J* = 8.3 Hz, 2 H), 7.59 (dd, *J* = 7.8, 1.5 Hz, 2 H), 7.63 - 7.39 (m, Hz, 4 H), 7.47 (t, *J* = 8.0 Hz, 2 H), 7.44 (dt, *J* = 8.5, 4.5 Hz, 2 H), 7.04 (dt, *J* = 7.8, 1.3 Hz, 2 H),

3.25 (q,  $J = 6.5$  Hz, 4 H), 1.52 (s, 4 H), 1.41 - 1.22 (m, 8 H).  $^{13}\text{C}$  NMR (DMSO- $d_6$ , 100 MHz):  $\delta$  168.1, 153.4, 139.4, 134.3, 133.8, 130.9, 128.1, 127.7, 125.8, 125.6, 125.4, 124.0, 122.6, 122.3, 121.1, 121.0, 120.4, 28.9, 28.7, 26.5. MS (FAB $^+$ ): 721 [M+H] $^+$ . HRMS (FAB $^+$ ): Calculated for  $\text{C}_{44}\text{H}_{45}\text{N}_6\text{O}_4$ : 721.3502; Found: 721.3603.

#### *Synthesis of alkyl bis(3-nitrobenzamide) compounds*

In a single neck round bottom flask, 3.4 g (18.3 mmol) of 3-nitrobenzoyl chloride were dissolved in 183 mL of dry THF with stirring under Ar atmosphere for 15 min. Then, 8.3 mmol of alkyl diamine (3, 4, 6 and 8 carbons) and 0.3 mL of triethylamine were added to the solution. The reaction was stirred for 24 h. Then, the solvent was removed by heating under reduced pressure and the product was washed and filtered as many times as needed to give an analytically pure solid compound.

*N,N'*-(propane-1,3-diyl)bis(3-nitrobenzamide) (**A**). White solid. Yield: 90.5%. M. p. 210-212 °C. FT-IR: 3363, 3098, 2945, 2874, 1637, 1548, 1524, 1471  $\text{cm}^{-1}$ .  $^1\text{H}$  NMR (DMSO- $d_6$ , 400 MHz):  $\delta$  8.93 (t,  $J = 5.5$  Hz, 2 H), 8.68 (t,  $J = 2.0$  Hz, 2 H), 8.38 (ddd,  $J = 8.0, 2.0, 1.0$  Hz, 2 H), 8.31 (td,  $J = 8.0, 2.0$  Hz, 2 H), 7.78 (t,  $J = 8.0$  Hz, 2 H), 3.46 - 3.36 (m, 4 H), 1.87 (qnt,  $J = 6.9$  Hz, 2 H).  $^{13}\text{C}$  NMR (DMSO- $d_6$ , 100 MHz):  $\delta$  164.0, 147.7, 135.9, 133.5, 130.0, 125.7, 121.8, 37.4, 28.7. MS (FAB $^+$ ): 373 [M+H] $^+$ . HRMS (FAB $^+$ ): Calculated for  $\text{C}_{17}\text{H}_{17}\text{N}_4\text{O}_6$ : 373.1148; Found: 373.1143.

*N,N'*-(butane-1,4-diyl)bis(3-nitrobenzamide) (**B**). White solid. Yield: 80.3%. M. p. 242-244 °C. FT-IR: 3361, 3091, 2937, 2861, 1637, 1551, 1523, 1478  $\text{cm}^{-1}$ .  $^1\text{H}$  NMR (DMSO- $d_6$ , 400 MHz):  $\delta$  8.87 (t,  $J = 5.4$  Hz, 2 H), 8.67 (t,  $J = 2.0$  Hz, 2 H), 8.37 (ddd,  $J = 0.7, 2.0, 8.1$  Hz, 1 H), 8.29 (td,  $J = 1.2, 8.1$  Hz, 2 H), 7.77 (t,  $J = 8.1$  Hz, 2 H), 3.39 - 3.26 (m, 4 H), 1.66 - 1.56 (m, 4 H).  $^{13}\text{C}$  NMR (DMSO- $d_6$ , 100 MHz):  $\delta$  163.8, 147.6, 135.9, 133.5, 130.0, 125.6, 121.7, 33.6, 26.4. MS (FAB $^+$ ): 387 [M+H] $^+$ . HRMS (FAB $^+$ ): Calculated for  $\text{C}_{18}\text{H}_{19}\text{N}_4\text{O}_6$ : 387.1305; Found: 387.1310.

*N,N'*-(hexane-1,6-diyl)bis(3-nitrobenzamide) (**C**). White solid. Yield: 59%. M. p. 192-194 °C. FT-IR: 3309, 3100, 2935, 2873, 1629, 1577, 1530, 1478  $\text{cm}^{-1}$ .  $^1\text{H}$  NMR (DMSO- $d_6$ , 400 MHz):  $\delta$  8.83 (t,  $J = 5.4$  Hz, 2 H), 8.67 (t,  $J = 2.0$  Hz, 2 H), 8.37 (ddd,  $J = 8.1, 2.3, 1.0$  Hz, 2 H), 8.28 (td,  $J = 8.1, 1.3$  Hz, 2 H), 7.77 (t,  $J = 8.1$  Hz, 2 H), 3.38 - 3.24 (m, 4 H), 1.63 - 1.47 (m, 4 H), 1.46 - 1.30 (m, 4 H).  $^{13}\text{C}$  NMR (DMSO- $d_6$ , 100

MHz):  $\delta$  163.8, 147.7, 135.9, 133.5, 130.0, 125.6, 121.8, 39.3, 28.8, 26.1. MS (FAB<sup>+</sup>): 415 [M+H]<sup>+</sup>. HRMS (FAB<sup>+</sup>): Calculated for C<sub>20</sub>H<sub>23</sub>N<sub>4</sub>O<sub>6</sub>: 415.4260; Found: 415.1628.

*N,N'*-(octane-1,8-diyl)bis(3-nitrobenzamide) (**D**). White solid. Yield: 59%. M. p. 178-180 °C. FT-IR: 3312, 3100, 2932, 2872, 1629, 1577, 1530, 1477 cm<sup>-1</sup>. <sup>1</sup>H NMR (DMSO-*d*<sub>6</sub>, 400 MHz):  $\delta$  8.81 (s, 2 H), 8.66 (s, 2 H), 8.28 (d, *J* = 7.3 Hz, 2 H), 8.37 (d, *J* = 8.1 Hz, 2 H), 7.77 (t, *J* = 7.3 Hz, 2 H), 1.55 (m, 4 H), 1.43 - 1.17 (m, 8 H). <sup>13</sup>C NMR (DMSO-*d*<sub>6</sub>, 100 MHz):  $\delta$  161.9, 148.2, 134.1, 130.5, 126.2, 122.3, 114.2, 33.3 29.4, 29.2, 26.9 MS (FAB<sup>+</sup>): 443 [M+H]<sup>+</sup>. HRMS (FAB<sup>+</sup>): Calculated for C<sub>22</sub>H<sub>27</sub>N<sub>4</sub>O<sub>6</sub>: 443.1931; Found: 443.1889.

#### *Synthesis of alkyl bis(3-aminobenzamide) compounds*

In a single neck round bottom flask, Pd/C at 10% and the corresponding alkyl bis(3-nitrobenzamide) (**A**, **B**, **C** o **D**) were placed. The flask was purged with an Ar atmosphere. Then, dry MeOH (10 mL × 1 mmol) was added. The Ar atmosphere was replaced by a hydrogen atmosphere and the reaction was stirred for 24 h. Then, the mixture was filtered to separate the catalyst and the solvent was removed by heating under reduced pressure, to give an analytical pure product.

*N,N'*-(propane-1,3-diyl)bis(3-aminobenzamide) (**m3**). Brown solid. Yield: 97.8%. M. p. 98-100 °C. FT-IR: 3324, 3226, 3063, 2931, 1622, 1579, 1528, 1487 cm<sup>-1</sup>. <sup>1</sup>H NMR (DMSO-*d*<sub>6</sub>, 400 MHz):  $\delta$  8.29 (t, *J* = 5.7 Hz, 2 H), 7.08 (t, *J* = 7.7 Hz, 2 H), 7.05 (s, 2 H), 6.96 (d, *J* = 7.7 Hz, 2 H), 6.69 (ddd, *J* = 7.7, 2.4, 1.0 Hz, 2 H), 5.22 (brs, 4 H), 3.35 - 3.20 (m, 4 H). <sup>13</sup>C NMR (DMSO-*d*<sub>6</sub>, 100 MHz):  $\delta$  167.5, 149.1, 136.0, 129.1, 116.8, 114.6, 113.2, 37.2, 29.8. MS (FAB<sup>+</sup>): 313 [M+H]<sup>+</sup>. HRMS (FAB<sup>+</sup>): Calculated for C<sub>17</sub>H<sub>21</sub>N<sub>4</sub>O<sub>2</sub>: 313.1665; Found: 313.1599.

*N,N'*-(butane-1,4-diyl)bis(3-aminobenzamide) (**m4**). Orange solid. Yield: 69.2%. M. p. 120-122 °C. FT-IR: 3433, 3332, 3222, 3057, 2943, 2866, 1647, 1583, 1547, 1520 cm<sup>-1</sup>. <sup>1</sup>H NMR (DMSO-*d*<sub>6</sub>, 400 MHz):  $\delta$  8.23 (t, *J* = 5.5 Hz, 2 H), 7.04 (t, *J* = 7.5 Hz, 2 H), 7.01 (s, 2 H), 6.94 (ddd, *J* = 7.5, 2.7, 1.1 Hz, 2 H), 6.67 (ddd, *J* = 7.5, 2.4, 1.3 Hz, 2 H), 5.21 (brs, 4 H), 3.32 - 3.12 (m, 4 H), 1.52 (brs, 4 H). <sup>13</sup>C NMR (DMSO-*d*<sub>6</sub>, 100 MHz): 166.9, 148.6, 135.7, 128.5, 116.2, 114.2, 112.8, 26.8, 23.9.

MS (FAB<sup>+</sup>): 327 [M+H]<sup>+</sup>. HRMS (FAB<sup>+</sup>): Calculated for C<sub>18</sub>H<sub>23</sub>N<sub>4</sub>O<sub>2</sub>: 327.1821; Found: 327.1820.

*N,N'*-(hexane-1,6-diyl)bis(3-aminobenzamide) (**m6**). Pink solid. Yield: 80.3%. M. p. 100-102 °C. FT-IR: 3390, 3324, 3218, 3054, 2928, 2854, 1625, 1582, 1533, 1489 cm<sup>-1</sup>. <sup>1</sup>H NMR (DMSO-*d*<sub>6</sub>, 400 MHz): δ 8.18 (t, *J* = 5.6 Hz, 2 H), 7.00 (t, *J* = 7.6 Hz, 2 H), 7.01 (s, 2 H), 6.92 (td, *J* = 7.6, 0.5 Hz, 2 H), 6.66 (ddd, *J* = 7.6, 2.0, 1.0 Hz, 2 H), 5.19 (s, 4 H), 3.31 - 3.08 (m, 4 H), 1.63 - 1.40 (m, 4 H), 1.31 (brs, 4 H). <sup>13</sup>C NMR (DMSO-*d*<sub>6</sub>, 100 MHz): δ 166.9, 148.6, 135.8, 128.5, 116.2, 114.2, 112.8, 39.0, 29.2, 26.3. MS (FAB<sup>+</sup>): 355 [M+H]<sup>+</sup>. HRMS (FAB<sup>+</sup>): Calculated for C<sub>20</sub>H<sub>27</sub>N<sub>4</sub>O<sub>2</sub>: 355.2134; Found: 355.2143.

*N,N'*-(octane-1,8-diyl)bis(3-aminobenzamide) (**m8**). Beige solid. Yield: 90.4%. M. p. 120-122 °C. FT-IR: 3393, 3349, 3208, 3054, 2926, 2853, 1625, 1583, 1538, 1490 cm<sup>-1</sup>. <sup>1</sup>H NMR (DMSO-*d*<sub>6</sub>, 400 MHz): δ 8.17 (t, *J* = 5.5 Hz, 2 H), 7.15 - 6.85 (d, *J* = 7.8 Hz, 2 H), 7.01 (s, 2 H), 6.92 (dd, *J* = 7.8, 1.2 Hz, 2 H), 6.66 (td, *J* = 7.8, 1.1 Hz, 1 H), 5.19 (brs, 4 H), 3.19 (q, *J* = 6.5 Hz, 4 H), 1.58 - 1.39 (m, 4 H), 1.28 (s, 8 H). <sup>13</sup>C NMR (DMSO-*d*<sub>6</sub>, 100 MHz): δ 166.9, 148.6, 135.8, 128.5, 116.2, 114.2, 112.9, 29.2, 28.8, 26.5. MS (FAB<sup>+</sup>): 383 [M+H]<sup>+</sup>. HRMS (FAB<sup>+</sup>): Calculated for C<sub>22</sub>H<sub>31</sub>N<sub>4</sub>O<sub>2</sub>: 383.2447; Found: 383.2469.

#### *Synthesis of N,N'*-alkyl bis(3-(3-(naphthalen-1-yl)ureyl)benzamide) compounds

In a single neck round bottom flask, 2.2 equivalents of 1-naphthyl isocyanate were added to a stirred solution of an alkyl bis(3-aminobenzamide) (1 equivalent of **m3**, **m4**, **m6** or **m8**) in dry THF under Ar atmosphere. Then, the reaction mixture was stirred for 24 h at RT and the solvent was removed by heating under reduced pressure. The product was washed and filtered as many times as needed to give an analytically pure solid compound.

*N,N'*-(propane-1,3-diyl)bis(3-(3-(naphthalen-1-yl)ureyl)benzamide) (**m3N**). Purple solid. Yield: 67.9%. M. p. 218-220 °C. FT-IR: 3271, 3054, 2956, 2935, 1720, 1634, 1585, 1528 cm<sup>-1</sup>. <sup>1</sup>H NMR (DMSO-*d*<sub>6</sub>, 400 MHz): δ 9.21 (s, 2 H), 8.78 (s, 2 H), 8.48 (t, *J* = 5.5 Hz, 2 H), 8.13 (d, *J* = 8.4 Hz, 2 H), 8.02 (d, *J* = 7.4 Hz, 2 H), 7.94 (d, *J* = 2.1 Hz, 2 H), 7.98 - 7.89 (m, 2 H), 7.70 (dd, *J* = 7.9, 0.9 Hz, 2 H), 7.65 (d, *J* = 8.2 Hz, 2 H), 7.60 (dt, *J* = 7.1, 1.0 Hz, 2 H), 7.54 (dt, *J* = 7.0, 0.7 Hz, 2 H), 7.48 (t, *J* = 7.9 Hz, 2 H), 7.47

(d,  $J = 7.8$  Hz, 2 H), 7.40 (t,  $J = 8.4$  Hz, 2 H), 3.45 - 3.36 (m, 4 H), 1.81 (qnt,  $J = 6.8$  Hz, 2 H).  $^{13}\text{C}$  NMR (DMSO- $d_6$ , 100 MHz):  $\delta$  166.2, 139.8, 135.4, 134.0, 133.6, 128.7, 128.3, 125.9, 125.8, 125.7, 123.0, 121.2, 120.5, 120.2, 117.5, 117.2, 37.0, 29.2. MS (FAB $^+$ ): 651 [M+H] $^+$ . HRMS (FAB $^+$ ): Calculated for  $\text{C}_{39}\text{H}_{35}\text{N}_6\text{O}_4$ : 651.2720; Found: 651.2735.

*N,N'*-(butane-1,4-diyl)bis(3-(3-(naphthalen-1-yl)ureyl)benzamide) (**m4N**). Beige solid. Yield: 54.7%. M. p. 234-236 °C. FT-IR: 3271, 3054, 2961, 2936, 1637, 1585, 1537  $\text{cm}^{-1}$ .  $^1\text{H}$  NMR (DMSO- $d_6$ , 400 MHz):  $\delta$  9.21 (s, 2 H), 8.78 (s, 2 H), 8.46 (t,  $J = 5.6$  Hz, 2 H), 8.13 (d,  $J = 8.6$  Hz, 2 H), 8.02 (d,  $J = 7.6$  Hz, 2 H), 7.98 - 7.90 (m, 4 H), 7.70 (dd,  $J = 8.1, 1.2$  Hz, 2 H), 7.65 (d,  $J = 8.3$  Hz, 2 H), 7.61 - 7.49 (m, 4 H), 7.49 - 7.43 (m, 4 H), 7.38 (t,  $J = 8.1$  Hz, 2 H), 3.33 - 3.23 (m, 4 H), 1.60 (brs, 4 H).  $^{13}\text{C}$  NMR (DMSO- $d_6$ , 100 MHz):  $\delta$  166.1, 152.8, 139.7, 135.5, 134.1, 133.7, 133.6, 128.6, 128.3, 125.9, 125.8, 125.7, 125.6, 123.0, 121.2, 120.3, 117.4, 117.3, 117.2, 38.9, 26.6. MS (FAB $^+$ ): 651 [M+H] $^+$ . HRMS (FAB $^+$ ): Calculated for  $\text{C}_{39}\text{H}_{35}\text{N}_6\text{O}_4$ : 651.2720; Found: 651.2768.

*N,N'*-(hexane-1,6-diyl)bis(3-(3-(naphthalen-1-yl)ureyl)benzamide) (**m6N**). Pink solid. Yield: 59.7%. M. p. 222-224 °C. FT-IR: 3282, 3081, 3054, 2932, 2856, 1637, 1629, 1586, 1543  $\text{cm}^{-1}$ .  $^1\text{H}$  NMR (DMSO- $d_6$ , 400 MHz):  $\delta$  9.20 (s, 2 H), 8.78 (s, 2 H), 8.43 (t,  $J = 5.6$  Hz, 2 H), 8.13 (d,  $J = 8.6$  Hz, 2 H), 8.02 (dd,  $J = 7.7, 1.1$  Hz, 2 H), 7.98 - 7.88 (m, 4 H), 7.69 (ddd,  $J = 8.1, 2.2, 1.0$  Hz, 1 H), 7.65 (d,  $J = 8.1$  Hz, 2 H), 7.61 - 7.49 (m, 6 H), 7.49 - 7.42 (m, 4 H), 7.38 (t,  $J = 7.8$  Hz, 2 H), 3.27 (q,  $J = 6.8$  Hz, 4 H), 1.55 (s, 4 H), 1.44 - 1.29 (m, 4 H).  $^{13}\text{C}$  NMR (DMSO- $d_6$ , 100 MHz):  $\delta$  166.4, 153.1, 140.0, 135.9, 134.6, 133.9, 133.9, 128.6, 126.2, 126.1, 126.1, 126.0, 125.9, 123.3, 123.1, 121.6, 121.5, 120.7, 120.5, 117.7, 117.6, 117.5, 39.4, 29.3, 26.5. MS (FAB $^+$ ): 693 [M+H] $^+$ . HRMS (FAB $^+$ ): Calculated for  $\text{C}_{42}\text{H}_{41}\text{N}_6\text{O}_4$ : 693.3189; Found: 693.3278.

*N,N'*-(octane-1,8-diyl)bis(3-(3-(naphthalen-1-yl)ureyl)benzamide) (**m8N**). Pink solid. Yield: 69.0%. M. p. 188-190 °C. FT-IR: 3278, 3053, 2930, 2854, 1636, 1628, 1586, 1543  $\text{cm}^{-1}$ .  $^1\text{H}$  NMR (DMSO- $d_6$ , 400 MHz):  $\delta$  9.20 (s, 2 H), 8.78 (s, 2 H), 8.41 (t,  $J = 5.6$  Hz, 2 H), 8.13 (d,  $J = 8.1$  Hz, 2 H), 8.02 (dd,  $J = 7.6, 1.0$  Hz, 2 H), 7.98 - 7.88 (m, 4 H), 7.69 (ddd,  $J = 8.1, 2.2, 1.0$  Hz, 3 H), 7.65 (d,  $J = 8.3$  Hz, 2 H), 7.63 - 7.49 (m, 4 H), 7.49 - 7.41 (m, 4 H), 7.38 (t,  $J = 7.8$  Hz, 2 H), 3.25 (q,  $J = 6.1$  Hz, 4 H), 1.61 - 1.42 (m, 4 H), 1.32 (s, 8 H).  $^{13}\text{C}$  NMR (DMSO- $d_6$ , 100 MHz):  $\delta$  165.9, 152.7, 139.6, 135.4, 134.1, 134.0, 133.5, 133.5, 128.5, 128.2, 125.8, 125.7, 125.6, 125.5, 122.8, 122.7,

121.2, 121.1, 120.3, 117.3, 117.2, 117.1, 39.0, 28.9, 28.6, 26.3. MS (FAB<sup>+</sup>): 721 [M+H]<sup>+</sup>. HRMS (FAB<sup>+</sup>): Calculated for C<sub>44</sub>H<sub>45</sub>N<sub>6</sub>O<sub>4</sub>: 721.3502; Found: 721.3503.

## Results and discussion

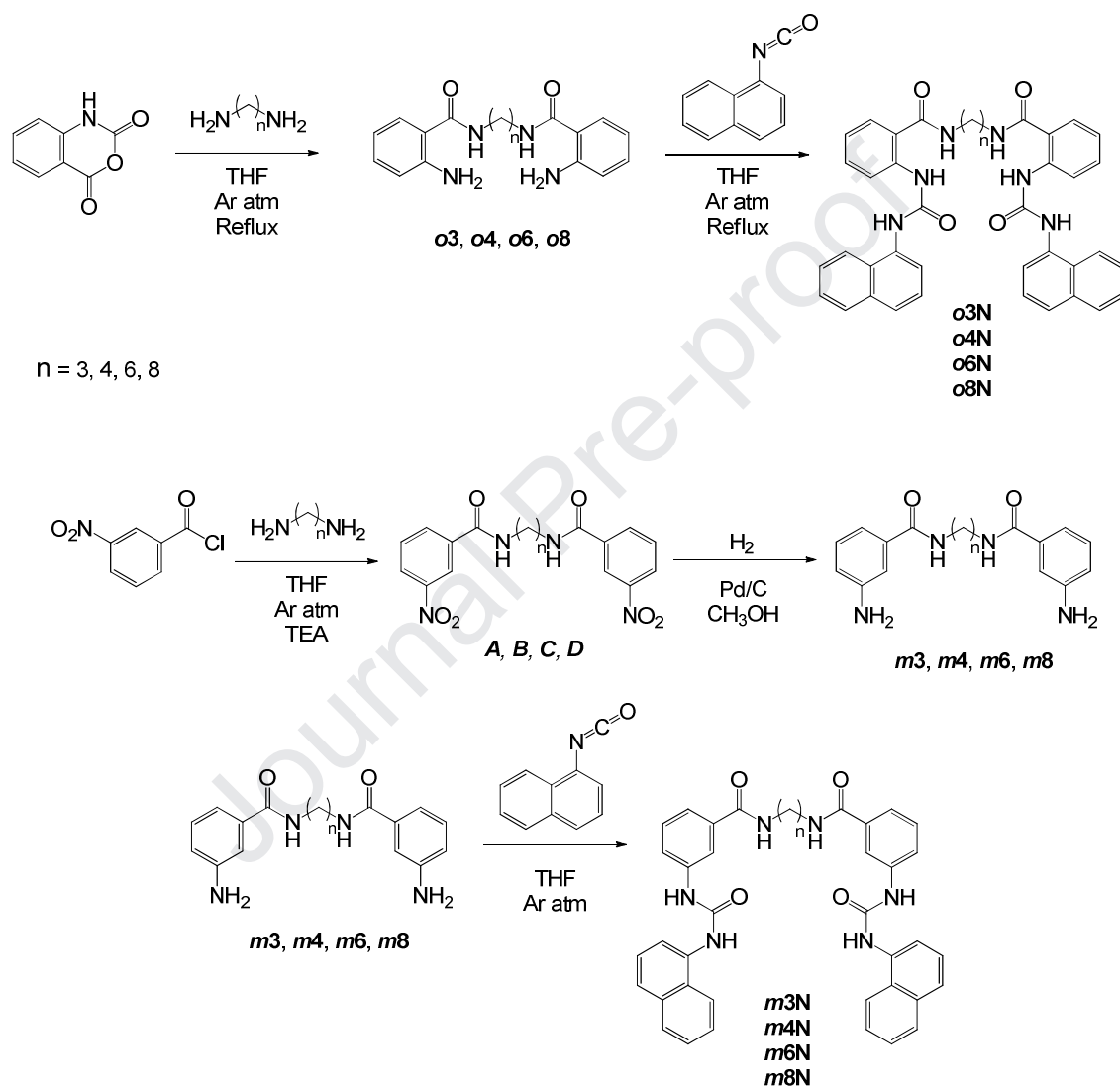
### Synthesis

The synthetic routes for **o(3-8)N** and **m(3-8)N** receptors are shown in Scheme 1. First, 2.2 equivalents of isatoic anhydride were treated with 1.0 equivalent of alkyl diamine (3, 4, 6 and 8 carbons) to obtain the alkyl bis(2-aminobenzamide)s **o(3-8)**. Then, the alkyl bis(2-aminobenzamide)s **o(3-8)**, were treated with 2.2 equivalents of 1-naphthyl isocyanate to afford the **o(3-8)N** receptors. In other synthetic route, 2.2 equivalents of *m*-nitrobenzoyl chloride were treated with 1.0 equivalent of alkyl diamine to obtain the corresponding alkyl bis(3-nitrobenzamide)s **A-D**. Then, a nitro-reduction of **A-D** compounds under H<sub>2</sub> atmosphere gave the alkyl bis(3-aminobenzamide)s **m(3-8)**, and finally the addition of 2.2 equivalents of 1-naphthyl isocyanate led to **m(3-8)N** receptors.

All receptors in *ortho* and *meta* position were characterized by infrared spectroscopy (FTIR), nuclear magnetic resonance (<sup>1</sup>H and <sup>13</sup>C NMR) and fast atom bombardment mass spectrometry (FAB-MS), and their chemical composition was verified by high-resolution mass spectrometry (HRMS). The IR spectra showed vibrations corresponding to the urea and amide N-H stretching between 3250 and 3300 cm<sup>-1</sup>. Also, two stretching vibrations for urea and amide carbonyls were found at 1640-1720 and 1620-1650 cm<sup>-1</sup>, respectively. The typical signal patterns of an *ortho* and *meta* substituted aromatic ring for **o(3-8)N** and **m(3-8)N** receptors were observed in the <sup>1</sup>H NMR spectra obtained in DMSO-*d*<sub>6</sub>. In addition, the signals for the naphthyl group in **o(3-8)N** and **m(3-8)N** receptors were assigned correctly.

The <sup>1</sup>H NMR spectra of *ortho* receptors show singlet signals at 10.29 and 9.60 ppm for urea hydrogens H<sub>f,f'</sub> and H<sub>g,g'</sub>, respectively, and a triplet signal in the range of 8.74-8.62 ppm for amide hydrogen H<sub>e,e'</sub>; whereas in *meta* receptors, the urea and amide hydrogens signals are located at 9.20 (H<sub>f,f'</sub>) and 8.78 (H<sub>g,g'</sub>) and 8.48-8.41 (H<sub>e,e'</sub>) ppm, respectively. This difference in chemical shifts for urea and amide hydrogens signals is caused by

structural features; the relative position of urea and benzamide groups and the resonance effect provided by the chromophore, are the main factors. The major effect was observed over the urea hydrogen ( $H_{g,g'}$ ) directly attached to the chromophore. On the other hand, the signal  $H_{f,f'}$  is the most shifted downfield, due to the resonance effect in the benzamide. Finally, the HRMS analysis confirmed the chemical composition for all compounds.



**Scheme 1.** Synthesis routes for alkyl bis(naphthylureylbenzamide)-based **o(3-8)N** and **m(3-8)N** receptors.

#### *Anion recognition by UV-Vis*

The **m(3-8)N** and **o(3-8)N** receptors have broad absorption bands due to the presence of an amino conjugated naphthyl group, with maximums at 296 and at 301-306 nm, respectively. These bands correspond to an auxochrome  $\pi-\pi^*$  electronic transition. The

supramolecular interaction of receptors was evaluated by titration with tetrabutylammonium salts, TBAX, where X = acetate (AcO), benzoate (BzO), dihydrogen phosphate (HP), fluoride (F) and hydrogen pyrophosphate (HPP) by UV-Vis in acetonitrile. The results showed significant changes in the absorption bands of **m(3-8)N** receptors. Figure 2a shows the absorption spectra of **m6N** with TBAF at different concentration. The absorption band at 296 nm shifted to 305 nm with an increase in absorbance (hyperchromic effect). In addition, two isosbestic points located in 275 and 294 nm are present. These changes indicate the supramolecular interaction between the receptor and the anion. All **m(3-8)N** receptors underwent a similar behavior towards TBAX salts (Figures S1-S4). The major response was observed with HPP. The spectral changes and sensibility of **m(3-8)N** towards the different anions were in the order  $\text{HPP} > \text{F} \approx \text{HP} > \text{AcO} > \text{BzO}$ , as seen in the absorbance profiles (Figure 2b). This behavior is directly related to the negative charges number and basicity of the anion. Interestingly, receptors **o(3-8)N** did not show significant changes with any of the selected anions for this study (Figures S5-S8). The behavior of **o(3-8)N** with TBAX salts is similar to the observed with a previously reported *N*-benzyl mono ureylbenzamide receptor.<sup>4</sup> The anion interacts with the urea hydrogens and a rotation of the amide carbonyl occurs, allowing the interaction of the anion and amide hydrogen. However, the conformational changes avoids the electronic conjugation from urea to naphthyl group, and the absorption band do not change during the titration. The coplanarity of the naphthyl-urea-benzamide system is conserved in **m(3-8)N** receptors when interact with anions, and the electronic transitions are affected.

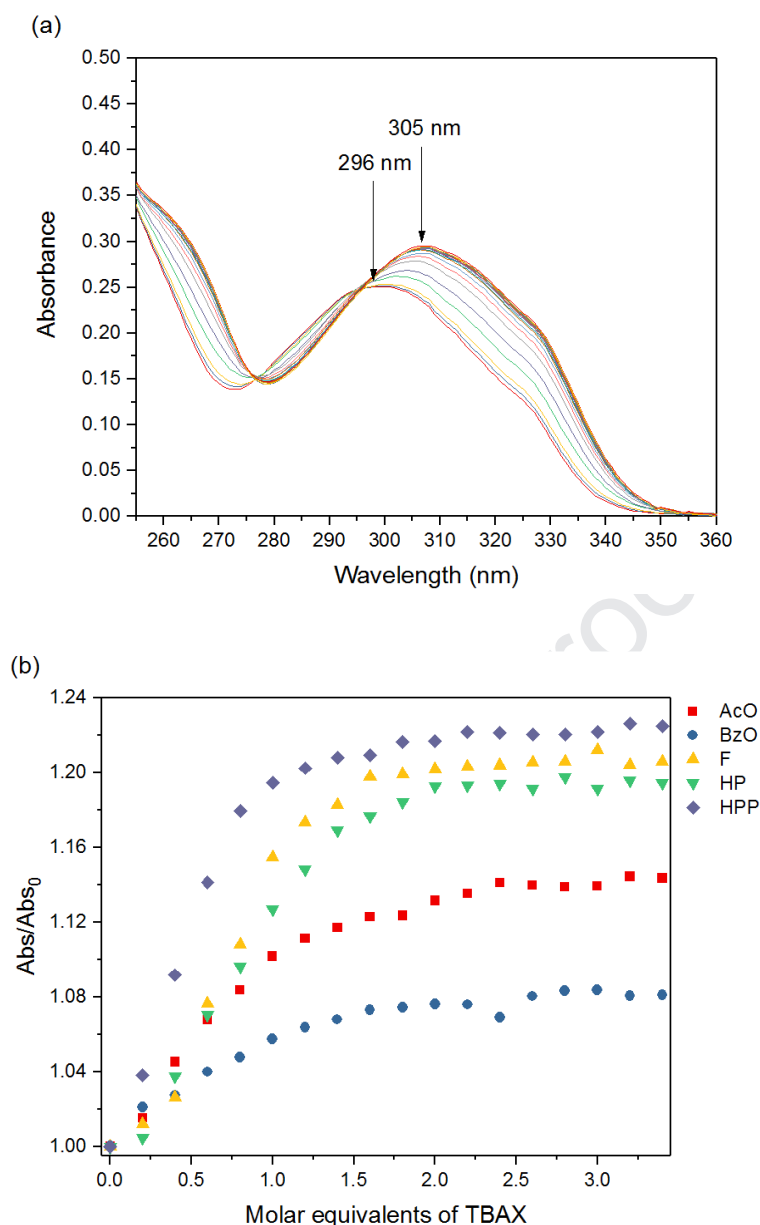


**Figure 2.** (a) UV-Vis spectra obtained in the titration of **m6N** [ $1 \times 10^{-5}$  M] with TBAF in acetonitrile. (b) Relative absorbance profiles obtained by titration of **m6N** with different TBAX salts,  $\lambda = 305$  nm.

It was possible to estimate the association constants  $K$  for the complexes using the absorbance data. A non-linear fit was used for a 1:1 interaction model, following the Equation 1 reported by Thordarson.<sup>33</sup>

Eqn. (1)

$$Abs_{obs} = Abs_H + 0.5\Delta Abs_{\infty} \left\{ \frac{[H]_T + [G]_T + \frac{1}{K} - \sqrt{\left([H]_T + [G]_T + \frac{1}{K}\right)^2 - 4[H]_T * [G]_T}}{[H]_T} \right\}$$

where  $A_{obs}$  is the complexed receptor absorbance,  $A_H$  is the free receptor absorbance,  $\Delta Abs_{\infty}$  is the maximum absorbance change induced by the presence of a given guest,  $[G]_T$  is the total concentration of guest,  $[H]_T$  is the total concentration of receptor, and  $K$  is the association constant. Table 1 lists the association constants for the complexes calculated from absorbance data using Equation 1 for a 1:1 interaction model. The  $K$  values were in the range of  $10^5$  to  $10^8$ . More refined calculations using HypSpec<sup>34-36</sup> program were performed, to analyze the data that did not fit with the Equation 1. The program confirmed the  $K$  values for 1:1 complexes, and provided the  $K$  values for 2:1 and 1:2 complexes (Table 1). The formation of 2:1 complexes was very interestingly considering that the typical behavior of the bis-urea receptors is the formation of 1:1 and 1:2 complexes. The presence of 2:1 complexes with AcO and HPP indicate that the anions may serve as template for the self-assembly of two receptor molecules at low concentration of anion, but the 1:1 complex is predominant when the anion concentration increases. Interestingly, only the 2:1 stoichiometry is detected for **m8N**-HPP complex (Figures S9 and S10). The  $K$  values were determined only for *meta* receptors due to the *ortho* receptors do not show significant change in the presence of TBAX salts.

**Table 1.** Association constants ( $K$ ) for **m(3-8)N** and anion complexes determined from UV-Vis data.

X	Ratio: R/A	<b>m3N</b> $K$ ( $M^{-1}$ )	<b>m4N</b> $K$ ( $M^{-1}$ )	<b>m6N</b> $K$ ( $M^{-1}$ )	<b>m8N</b> $K$ ( $M^{-1}$ )
AcO	<b>R<sub>2</sub>A</b>	<sup>b</sup> $1.9 \times 10^{12}$	<sup>b</sup> $1.7 \times 10^{14}$	<b>ND</b>	<b>ND</b>
	<b>RA</b>	<sup>b</sup> $3.1 \times 10^6$	<sup>b</sup> $1.1 \times 10^7$	<sup>a</sup> $3.4 \times 10^5$	<sup>a</sup> $3.7 \times 10^5$
	<b>RA<sub>2</sub></b>	<sup>b</sup> $9.3 \times 10^{10}$	<b>ND</b>	<b>ND</b>	<b>ND</b>
BzO	<b>RA</b>	<sup>b</sup> $4.1 \times 10^5$	$8.3 \times 10^5$	$2.7 \times 10^5$	$4.7 \times 10^5$
	<b>RA<sub>2</sub></b>	<sup>b</sup> $3.1 \times 10^9$	<b>ND</b>	<b>ND</b>	<b>ND</b>
F	<b>RA</b>	<sup>a</sup> $1.5 \times 10^7$	<sup>a</sup> $2.7 \times 10^5$	<sup>a</sup> $5.3 \times 10^6$	<sup>a</sup> $7.1 \times 10^5$
HP	<b>RA</b>	<sup>a</sup> $2.8 \times 10^7$	<sup>a</sup> $4.0 \times 10^6$	<sup>a</sup> $2.7 \times 10^5$	<sup>a</sup> $2.2 \times 10^6$
HPP	<b>R<sub>2</sub>A</b>	<b>ND</b>	<sup>b</sup> $6.3 \times 10^{16}$	<sup>b</sup> $2.5 \times 10^{17}$	<sup>b</sup> $1.1 \times 10^{11}$
	<b>RA</b>	<b>ND</b>	<sup>b</sup> $3.2 \times 10^8$	<sup>b</sup> $6.3 \times 10^8$	<b>ND</b>

**ND:** Not determined. According to the data obtained, a non-linear adjustment was not achieved, and the association constants could not be determined. **R:** Receptor. **A:** Anion. <sup>a</sup> Determined by Eqn. 1. <sup>b</sup> Determined by HypSpec refined calculation program.  $K$  values have  $M^{-2}$  unit for 2:1 and 1:2 complexes and  $M^{-1}$  for 1:1 complexes.

The  $K$  values are consistent with the experimental results, the highest values correspond to the **m(3-8)N** complexes with HPP, followed by F and HP. However, not all the  $K$  values were determined due to the strong anion-receptor interaction. In general, there is a tendency of  $K$  to decrease as the alkyl chain length increases. The  $K$  value changes as the geometry and size of the anion change, but the charge of the anion has a significant effect. The relative position of the amide and urea groups is determinant in the anion recognition and the association stability due to the steric effect. Moreover, the shape, size and basicity of the anion have a great influence in the recognition process and stability of the complexes.

#### *Anion recognition by fluorescence*

The fluorescence spectra of **m(3-8)N** and **o(3-8)N** receptors, as well as, their respective titrations with TBAX salts were obtained in acetonitrile (Figure S11-S18). All receptors showed broad fluorescence bands due to the presence of a naphthyl fluorophore attached to the urea group. The emission band for **m(3-8)N** receptors has a maximum intensity at 370 nm and **o(3-8)N** receptors at 398 nm. The **m(3-8)N** receptors are more fluorescent than **o(3-8)N** receptors, due to a greater electron delocalization from the urea towards the naphthyl group, whereas the **o(3-8)N** receptors display an inductive effect from the benzamide system over urea and naphthyl groups, causing a poor electron mobility towards the fluorophore.

All **m(3-8)N** receptors show a fluorescent response towards the anions under study. In most cases, the fluorescence emission spectra showed a decrease in intensity as the TBAX salt was added, indicating the interaction with the anion. The Figure 3(a) shows the fluorescence spectra obtained in the titration of **m6N** with TBAF. The fluorescence profiles showed an *ON/OFF* response in the order  $\text{AcO} > \text{F} > \text{HP} \approx \text{BzO}$  (Figure 3b).

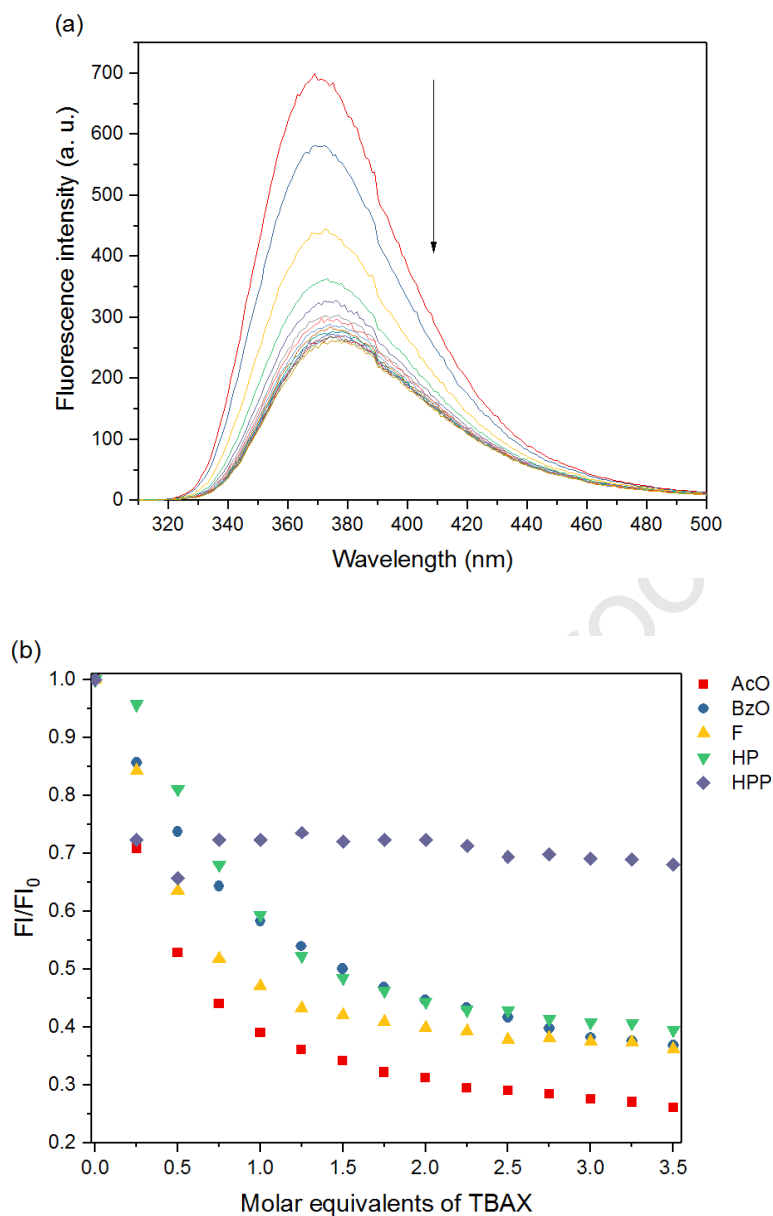


**Figure 3.** (a) Emission spectra obtained in the titration of **m6N** [ $1 \times 10^{-5}$  M] with TBAX in acetonitrile. (b) Relative fluorescence profiles of **m6N** with different TBAX salts,  $\lambda_{\text{ex}} = 302$  nm,  $\lambda_{\text{em}} = 370$  nm.

The fluorescence spectra of **m(3-8)N** receptors with HPP showed a different behavior from those observed with other TBAX salts (Figures 3b and 5). These receptors behave as  $ON^1/OFF/ON^2$  fluorescent probes in presence of HPP. First, there is a decrease in fluorescence intensity of **m(3-8)N** receptors when the addition of HPP reaches 0.5 equivalents (2:1 receptor-anion). Then, a partial increase in the intensity of a new emission band is observed, reaching its maximum intensity when 1.5 equivalents of HPP are added. Interestingly, this  $ON^1/OFF/ON^2$  response in fluorescence is more

evident in receptors with a shorter spacer as **m3N** and **m4N**. Figure 4 shows the fluorescence spectra of **m4N** at different concentrations of HPP.

This fluorescent response may be due to a more than one electronic process involved in the anionic recognition. The quenching of fluorescence is attributed to an electron-transfer (eT) process from the carbonyl oxygen of the urea, which assumes a partial negative charge in the interaction with the anion, facing the excited naphthyl group.<sup>14</sup> Electron density is transferred to the oxygen from the coordinated anion through H-bonds in this stage. Then a new band at 375 nm appears and shows an increase of fluorescence intensity after adding more than 0.5 equivalents. The increase of the new fluorescence band intensity is attributed to a charge transfer (cT) process, which occurs by deprotonation of urea. The red shift of the emission band (7 nm approx.) in **m(3-8)N** is induced by the complexation, and reflects the stabilization of the excited state by the H-bond interaction with the anion.<sup>37</sup> The fluorescence profiles of **m(3-8)N** show an  $ON^1/OFF/ON^2$  response with HPP in the order **m3N** > **m4N** > **m6N** > **m8N** (Figure 5). These results evidence the formation of 2:1 complexes with HPP, as well as, by electronic spectroscopy. The changes of fluorescence intensity indicate that the closeness of both ureylbenzamide units has an important influence over the spectroscopic response.

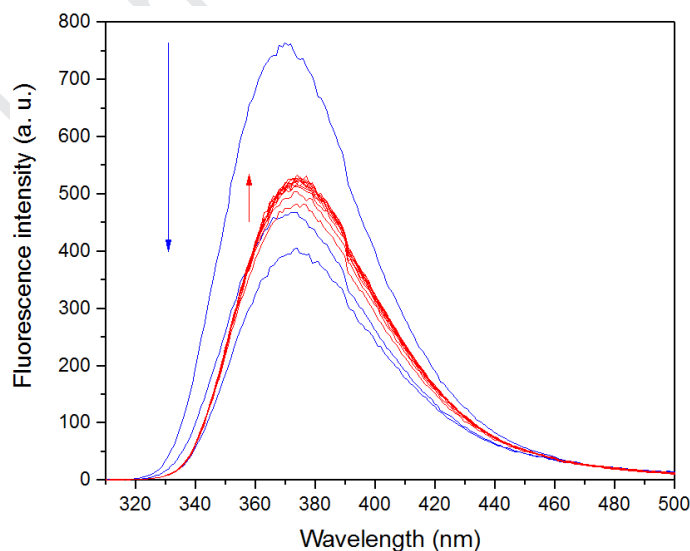


**Figure 4.** Emission spectra obtained in the titration of **m4N** [ $1 \times 10^{-5}$  M] with TBAHPP in acetonitrile.

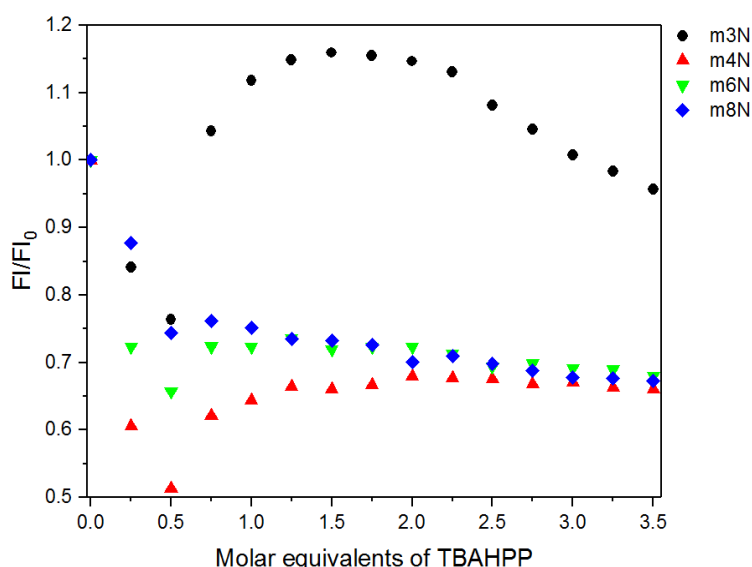


**Figure 5.** Relative fluorescence profiles obtained for **m(3-8)N** receptors with TBAHPP salt,  $\lambda_{\text{ex}} = 302 \text{ nm}$ ,  $\lambda_{\text{em}} = 370 \text{ nm}$ .

The data obtained from the fluorescence titrations were used to determine the association constants  $K$  of the supramolecular complexes. A non-linear fit was used for a 1:1 interaction model, this method is based on the same principle of Equation 1, and the difference is the use of fluorescence data, as depicted in Equation 2.

Eqn. (2)

$$F_{\text{obs}} = F_H + 0.5\Delta F_{\infty} \left\{ \frac{[H]_T + [G]_T + \frac{1}{K} - \sqrt{\left([H]_T + [G]_T + \frac{1}{K}\right)^2 - 4[H]_T * [G]_T}}{[H]_T} \right\}$$

where  $F_{\text{obs}}$  is the fluorescence intensity for the complex,  $F_H$  is the fluorescence intensity of the free receptor,  $\Delta F_{\infty}$  is the maximum fluorescence intensity change induced by the presence of a given guest,  $[G]_T$  is the total concentration of the guest,  $[H]_T$  is the total concentration of the receptor, and  $K$  is the association constant.

Table 2 lists the  $K$  values obtained from the emission data using Equation 2 for a 1:1 interaction model, which were in the range of  $10^3$  and  $10^6$ . More refined calculations using the HypSpec program were performed to analyze the data which did not fit with the Equation 2. The program confirmed the  $K$  values for 1:1 complexes, and provided the  $K$  values for 2:1 complexes with AcO and **m(3-8)N** receptors. There is a difference in the  $K$  values and stoichiometry estimated from the fitting of UV-Vis and fluorescence data for some complexes. This is hard to explain, but one plausible explanation is

related with the fact of that 2:1, 1:1 and 1:2 complexes have the same emission band, and as the 2:1 complex is formed first, the transformation to 1:1 and 1:2 complexes is not detected. It is believe that  $K$  values calculated from the UV-Vis data are more accurate, but the fitting of fluorescence data confirms the formation of 2:1 complexes.

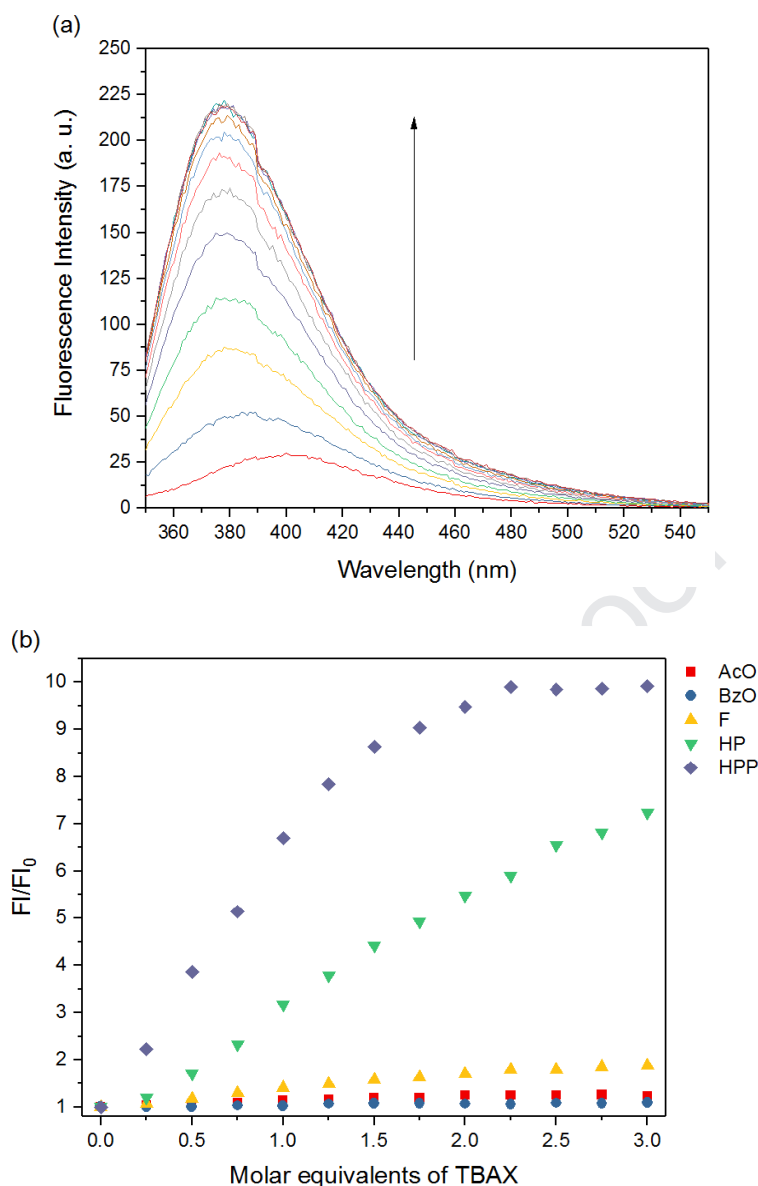
It is evident that magnitude of  $K$  is influenced by the length of the spacer alkyl chain. For example, there is a clear decrease of the  $K$  value in the complexes with HP as the alkyl chain length increases, and there is a similar tendency with the rest of anions. Moreover, the  $K$  values for supramolecular complexes of **m(3-8)N** and HPP could not be determined due to the high dispersion in the data, while the complexes with **o(3-8)N** receptors showed values in the range of  $10^4$  and  $10^7$ .

**Table 2.** Association constants ( $K$ ) for anion interaction with **m(3-8)N** and **o(3-6)N** receptors using the fluorescence data.

		<b>m3N</b>	<b>m4N</b>	<b>m6N</b>	<b>m8N</b>	<b>o3N</b>	<b>o4N</b>	<b>o6N</b>
X	R/A	$K$	$K$	$K$	$K$	$K$	$K$	$K$
AcO	<b>R<sub>2</sub>A</b>	<sup>b</sup> $5.7 \times 10^{11}$	<sup>b</sup> $3.3 \times 10^{11}$	<sup>b</sup> $1.0 \times 10^{11}$	<sup>b</sup> $1.0 \times 10^{12}$			
	<b>RA</b>	<sup>a</sup> $3.8 \times 10^6$	<sup>a</sup> $2.8 \times 10^6$	<sup>b</sup> $1.4 \times 10^5$	<sup>b</sup> $1.5 \times 10^6$	<sup>a</sup> $2.0 \times 10^4$	<sup>a</sup> $4.0 \times 10^5$	<sup>a</sup> $3.1 \times 10^4$
BzO	<b>R<sub>2</sub>A</b>	<sup>b</sup> $1.0 \times 10^{11}$				<b>ND</b>		
	<b>RA</b>	<sup>b</sup> $1.2 \times 10^6$	<sup>a</sup> $1.0 \times 10^6$	<sup>a</sup> $3.8 \times 10^5$	<sup>a</sup> $2.1 \times 10^5$	<b>ND</b>	<sup>a</sup> $1.4 \times 10^5$	<sup>a</sup> $5.2 \times 10^4$
F	<b>RA</b>	<sup>a</sup> $1.0 \times 10^6$	<sup>a</sup> $7.1 \times 10^6$	<sup>a</sup> $4.3 \times 10^6$	<sup>a</sup> $3.7 \times 10^5$	<sup>a</sup> $5.8 \times 10^3$	<b>ND</b>	<b>ND</b>
HP	<b>RA</b>	<sup>a</sup> $1.7 \times 10^6$	<sup>a</sup> $1.3 \times 10^6$	<sup>a</sup> $3.7 \times 10^5$	<sup>a</sup> $2.0 \times 10^5$	<b>ND</b>	<sup>a</sup> $1.3 \times 10^4$	<b>ND</b>
HPP	<b>RA</b>	<b>ND</b>	<b>ND</b>	<b>ND</b>	<b>ND</b>	<sup>a</sup> $4.1 \times 10^4$	<sup>a</sup> $8.3 \times 10^4$	<sup>b</sup> $2.8 \times 10^7$

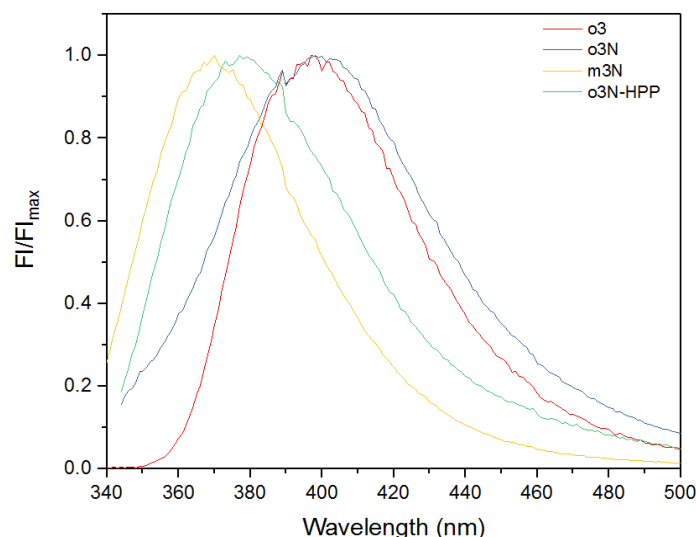
**ND:** Not determined. According to the obtained data a non-linear adjustment was not achieved, and therefore the association constants could not be determined. **R:** Receptor. **A:** Anion. <sup>a</sup> Determined by Eqn. 2. <sup>b</sup> Determined by HypSpec refined calculation program.  $K$  values have  $M^{-2}$  unit for 2:1 and 1:2 complexes and  $M^{-1}$  for 1:1 complexes.

The **o(3-8)N** receptors show an interesting *OFF/ON* fluorescent response in the titrations with TBAX salts. A shift of the emission band to shorter wavelength (20 nm approx.) is observed in the course of the titration. This change is more evident in **o3N** and **o4N** with HP and HPP salts (Figure 6 and Figure S14). This response is no longer observed as the length of the alkyl chain increases (Figures S13-S16).



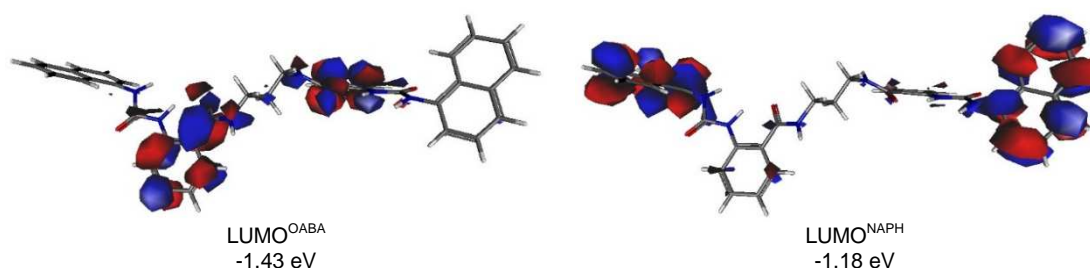
**Figure 6.** (a) Emission spectra obtained in the titration of **o3N** [ $1 \times 10^{-5}$  M] with TBAHPP in acetonitrile. (b) Relative fluorescence profiles obtained with different TBAX salts,  $\lambda_{\text{ex}} = 334$  nm,  $\lambda_{\text{em}} = 398$  nm.

The excitation and emission bands of **o3** and **o3N** have the same maximum excitation and emission wavelengths ( $\lambda_{\text{exc}} = 334$  nm y  $\lambda_{\text{em}} = 398$  nm), although the fluorescence intensity is lower for **o3N** (Figure 7). In addition, it was observed that the emission band of **o3N**-HPP complex has an emission band similar to **m3N**, where the fluorescence is due to the naphthyl fluorophore. These observations suggested a photoinduced electron transfer (PET) process between the naphthyl group (NAPH) and the *o*-aminobenzamide fragment (OABA). In a previous work, it was found that a PET process occurs if the OABA is conjugated with another fluorophore.<sup>38</sup>



**Figure 7.** Relative fluorescence profiles obtained for the receptors: **o3**, **o3N**, **m3N**, and the **o3N-HPP** supramolecular complex.

A theoretical study was carried out with DFT, a PBE0 functional and a DZVP base using the Gaussian 09 program.<sup>32</sup> The geometry of the receptor was optimized and the energy of the molecular orbitals (MOs) was calculated.<sup>32</sup> As a result, it was found that the MOs of naphthylurea fluorophore (HOMO-LUMO)<sup>NAPH</sup> have higher energy than the MOs of the *o*-aminobenzamide fluorophore (HOMO-LUMO)<sup>OABA</sup> (Figure 8). The (OABA-NAPH) dyad is irradiated at 334 nm and the OABA fluorophore is excited generating the <sup>1</sup>(OABA)<sup>\*</sup>-NAPH species. A photoinduced electron transfer (PET) from HOMO<sup>NAPH</sup> to the HOMO<sup>OABA</sup> is possible due to this MO is located in a superior position. Then, the OABA<sup>⊖</sup>-NAPH<sup>⊕</sup> specie is formed, and the energy emission is inactivated reducing the fluorescence intensity. The PET is inactivated in the complex and the emission of NAPH fluorophore is possible.



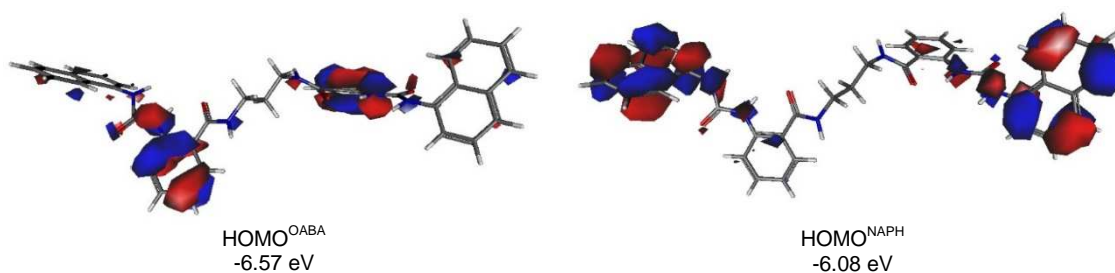


**Figure 8.** Molecular orbitals of **o3N** calculated by DFT.

The MO's energy in the receptor changes when it complexes with anions. The HOMO is located in the two naphthylurea units and the LUMO in the *o*-aminobenzamide units in the free receptor. Instead, the HOMO is located in the naphthylurea units and the LUMO orbital in the naphthyl group in the complexes; then a  $S_1 \rightarrow S_0$  transition or energy emission occurs in the naphthylurea fragment. This result is consistent with the emission wavelength observed for the complexes. Also, the MO's energy increases with the basicity and charge of the anion (Figure 9).

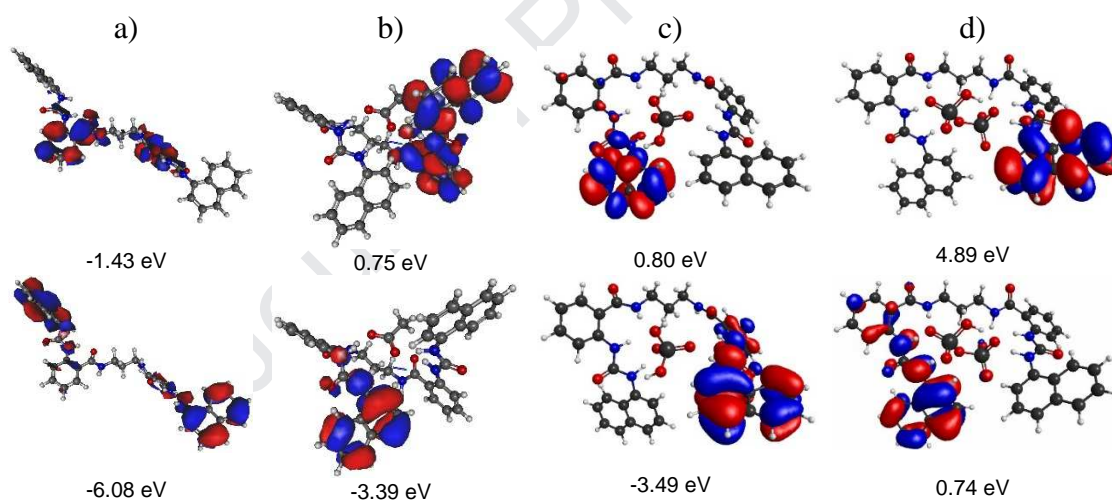


**Figure 9.** Distribution of the MOs in a) free **o3N**, b) **o3N-Ac**, c) **o3N-HP** and d) **o3N-HPP** complexes.

#### *Anion recognition study by $^1\text{H}$ NMR*

The  $^1\text{H}$  NMR titrations of receptors were performed to establish the interaction sites with different anions. For this purpose, it was decided to analyze two “short receptors” (**m3N** and **o3N**) and two “long receptors” (**m6N** and **o6N**) in order to detect an effect over the anion recognition process by the alkyl chain length. The main idea was to analyze the interaction of these receptors in a non-competitive solvent, which was

clearly possible at low concentration (0.01 mM) in acetonitrile. However, these receptors are insoluble in acetonitrile at high concentration (6 mM), thus the use of a polar solvent as DMSO was necessary in the studies by  $^1\text{H}$  NMR. The **m3N** and **m6N** receptors display spectral changes with all anions. The most affected hydrogens belong to the urea group,  $\text{H}_{\text{f},\text{f}'}$  and  $\text{H}_{\text{g},\text{g}'}$ , at 9.24 and 8.80 ppm, respectively. The recognition of AcO and BzO anions by **m3N** and **m6N** show a similar behavior (Figures S20-S22). The  $\text{H}_{\text{f},\text{f}'}$  and  $\text{H}_{\text{g},\text{g}'}$  signals shift to downfield about 2.67 and 2.48 ppm, respectively, after the addition of six equivalents of salt to a **m3N** solution in  $\text{DMSO-}d_6$  (Figure 10). The amide signal  $\text{H}_{\text{e},\text{e}'}$  at 8.52 ppm is not affected by AcO and BzO. Therefore, the amide is not involved in the anion recognition. Moreover, the singlet at 7.94 ppm which corresponds to  $\text{H}_{\text{d},\text{d}'}$  hydrogen shows a 0.18 ppm downfield shift. A doublet at 8.12 ppm corresponding to  $\text{H}_{\text{p},\text{p}'}$  shows a 0.19 ppm downfield shift. A 0.24 ppm up-field shift of  $\text{H}_{\text{h},\text{h}'}$  signal is due to the loss of the carbonyl effect over this hydrogen once the complex is formed. This chemical shift is caused by a change in the configuration and conjugation of the naphthyl with the urea group, giving a protective effect over  $\text{H}_{\text{h},\text{h}'}$  hydrogen (Figure 10).

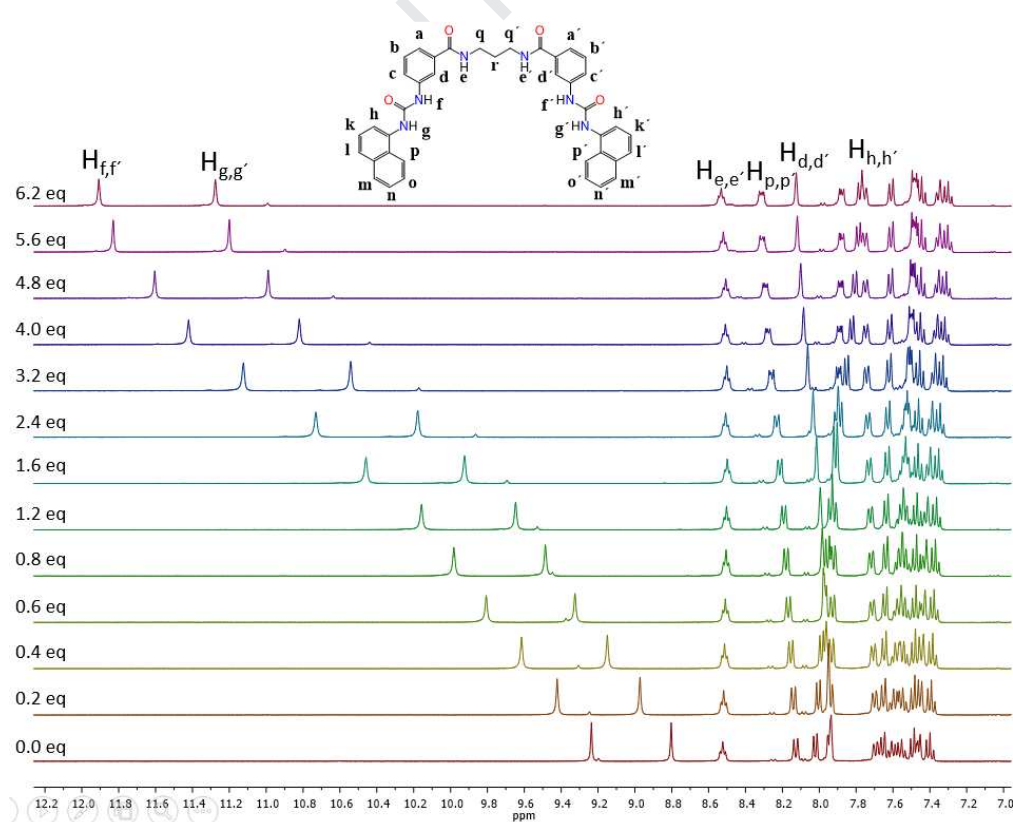


**Figure 10.** Partial  $^1\text{H}$  NMR spectra obtained in the titration of **m3N** [6 mM] with TBAAcO in  $\text{DMSO-}d_6$ .

The geometry of **m3N**, **m3N-AcO** and **m6N-AcO** were optimized using DFT, a PBE0 functional and a DZVP base, in order to visualize the interaction of these receptors with acetate (Figure 11). The ureylbenzamide units adopt a quasi-orthogonal position to minimize the distance of AcO and urea hydrogens in both complexes. Also, the naphthyl groups are oriented towards the acetate adopting an “*endo*” orientation to conserve the coplanarity of the naphthyl-urea-benzamide structure. The amide hydrogens are oriented to the anion, but the distance is unfavorable for an interaction. These geometries are consistent with the NMR experiments,  $H_{f,f'}$ ,  $H_{g,g'}$ ,  $H_{d,d'}$ ,  $H_{h,h'}$  and  $H_{p,p'}$  signals are the most affected in the interaction with AcO.

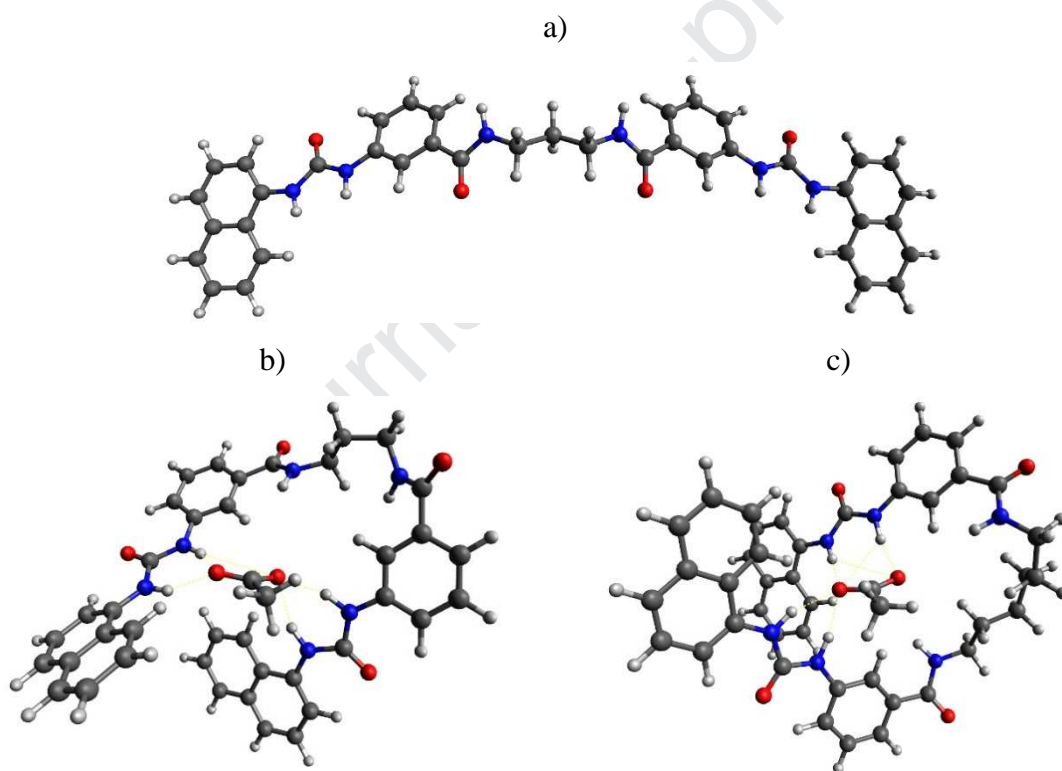


**Figure 11.** Optimized geometries of **m3N** (a), **m3N-AcO** complex (b) and **m6N-AcO** complex (c) by DFT.

The  $^1\text{H}$  NMR spectra of **m3N** and **m6N** with F show a downfield shift of  $H_{f,f'}$  and  $H_{g,g'}$  signals. Noteworthy, there is a significant shift of  $H_{e,e'}$  signal. The chemical shift of  $H_{e,e'}$  signal is constant until one molar equivalent of F added, then the signal shows a downfield shift about 1.16 ppm, evidencing the participation of the amide hydrogen in the recognition of a second F unit (Figure 12). The  $H_{d,d'}$  hydrogen gradually shifts to up-

field when F is added from zero to one equivalent, evidencing the electron-enrichment in the aromatic ring. Then, the signal shifts downfield indicating the interaction of this hydrogen with F. A previously reported *N*-benzyl mono ureylbenzamide receptor does not show a change in the amide signal, only the interaction with the urea hydrogens is observed.<sup>4</sup> Based on the changes of these signals, it is proposed the formation of a 1:1 complex where only the urea groups participate (Figure 13a). Then, the closeness of amide hydrogens in the 1:1 complex favors the interaction with a second F unit, forming a 1:2 complex, where  $H_{d,d'}$  hydrogens also participate (Figure 13b). In fact, the shift or broadening of the signals are less sensitive in **m6N-F** complex (Figure S23) indicating an important influence of the alkyl chain length in the recognition process of F. In addition, the  $H_{p,p'}$  signal is shifted 0.47 ppm downfield from its initial position due to the polarization of the aromatic C-H bond in the recognition of fluoride. The  $H_{h,h'}$ ,  $H_{k,k'}$  y  $H_{l,l'}$  signals corresponding to the naphthyl group also show different chemical environment produced by electronic and conformation changes.

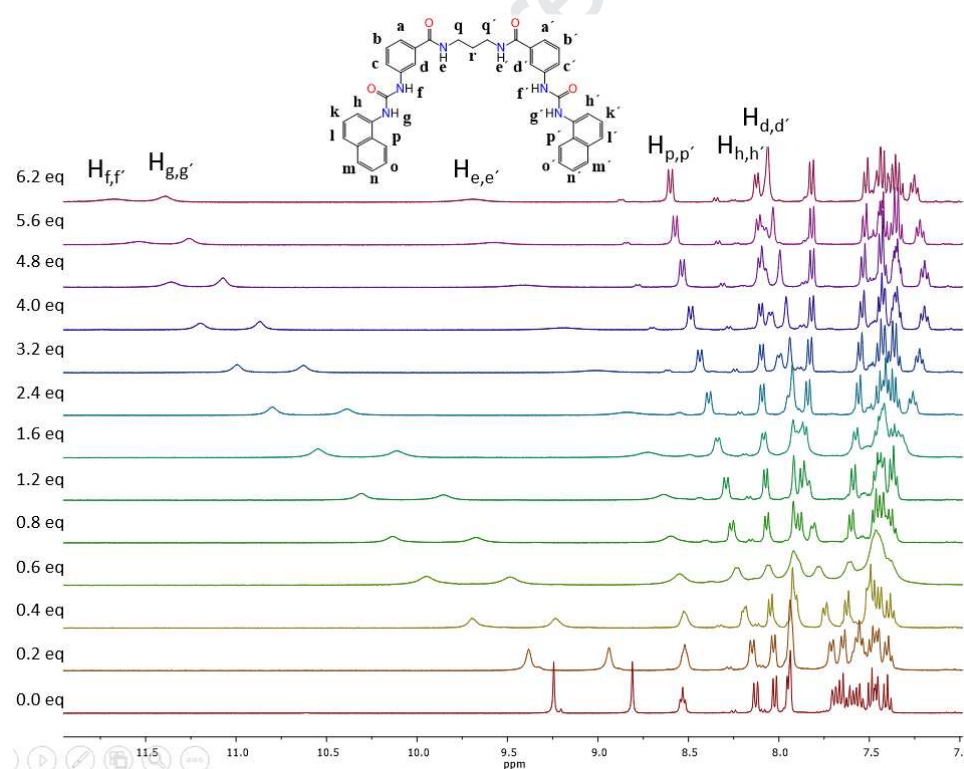


**Figure 12.** Partial  $^1\text{H}$  NMR spectra obtained in the titration of **m3N** [6 mM] with TBAF in  $\text{DMSO-}d_6$ .

a)

b)

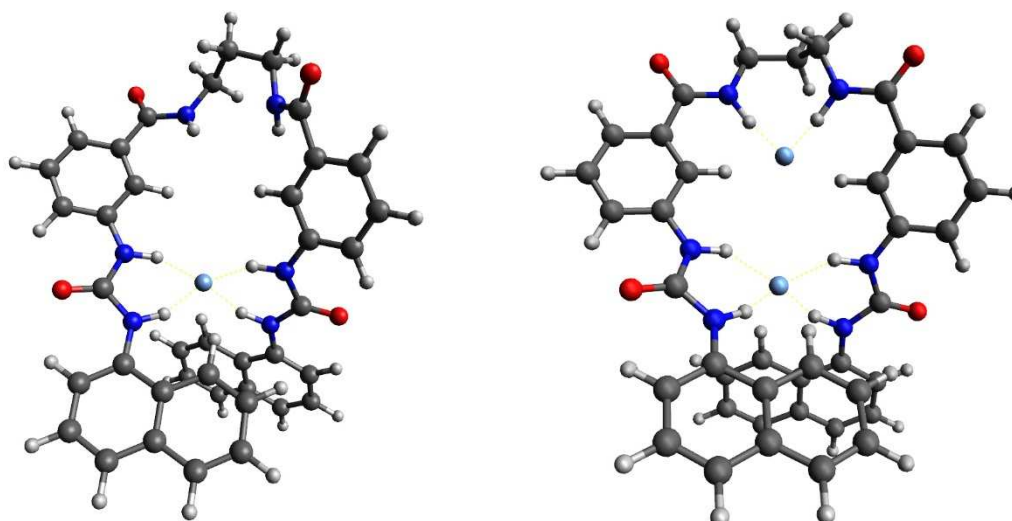


**Figure 13.** Optimized geometries of **m3N-F** (a) and **m3N-2F** (b) complexes by DFT.

The  $H_{f,f'}$  and  $H_{g,g'}$  signals have different chemical shift due to a different interaction strength or the possible formation of a multi-equivalent complexes with TBAHP. As depicted in Figure 14,  $H_{f,f'}$  signal shifts downfield more than  $H_{g,g'}$  since the first aliquot added. Then,  $H_{f,f'}$  signal shifts up-field when more than 2.4 molar equivalents are added, while the  $H_{g,g'}$  shifts gradually during the titration. The amide signal  $H_{e,e'}$  shifts slightly to downfield from zero to one equivalent of HP, but then becomes wide and shifts strongly when more HP is added. Interestingly, the  $H_{d,d'}$  signal, that normally shifts downfield, is constant from zero to 2.4 equivalents of HP, but then shifts up-field when more HP is added. All these changes in signals indicate that probably more than one HP unit interacts with the receptor.<sup>39-45</sup> The titration of **m6N** with HP shows an equal shift of the urea signals and the amide signal is less affected than in receptor **m3N** (Figure S24). The  $H_{d,d'}$  and  $H_{p,p'}$  signals shift to downfield as typically do with the rest of the anions. This is an example where the length of alkyl chain has a significant influence in the recognition process. Optimized geometries of **m3N-HP** and **m6N-HP** show the interaction of HP with receptors through multiple hydrogen bonds, where one amide and two urea groups participate (Figure 15).

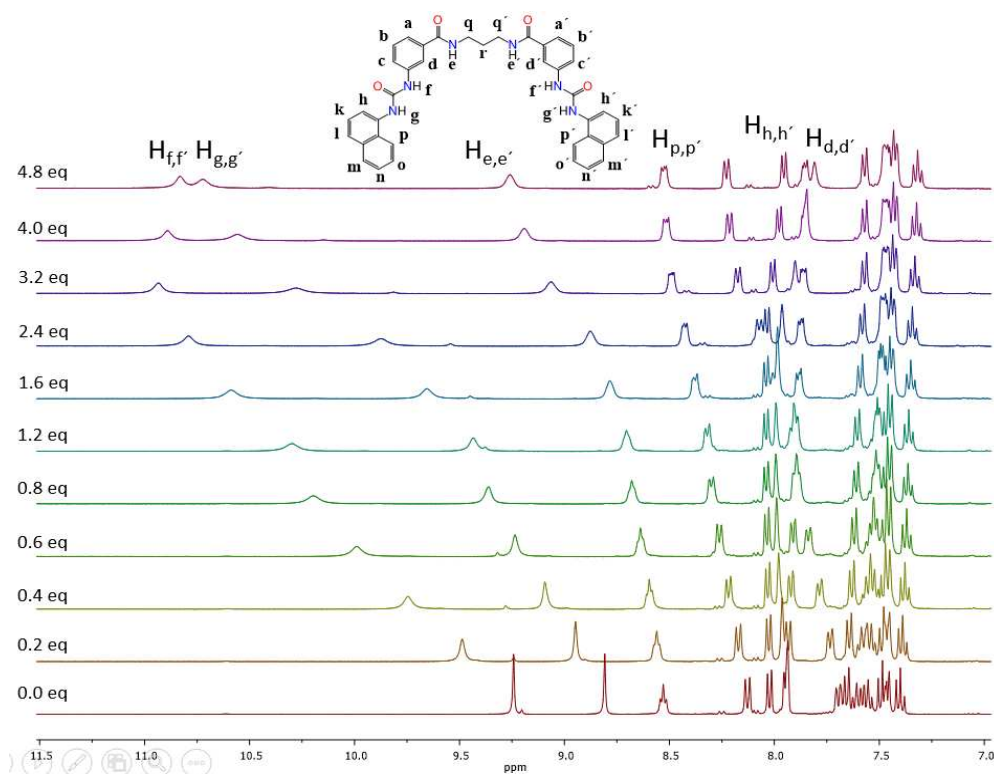


**Figure 14.** Partial  $^1\text{H}$  NMR spectra obtained in the titration of **m3N** [6 mM] with TBAHP in  $\text{DMSO-}d_6$ .

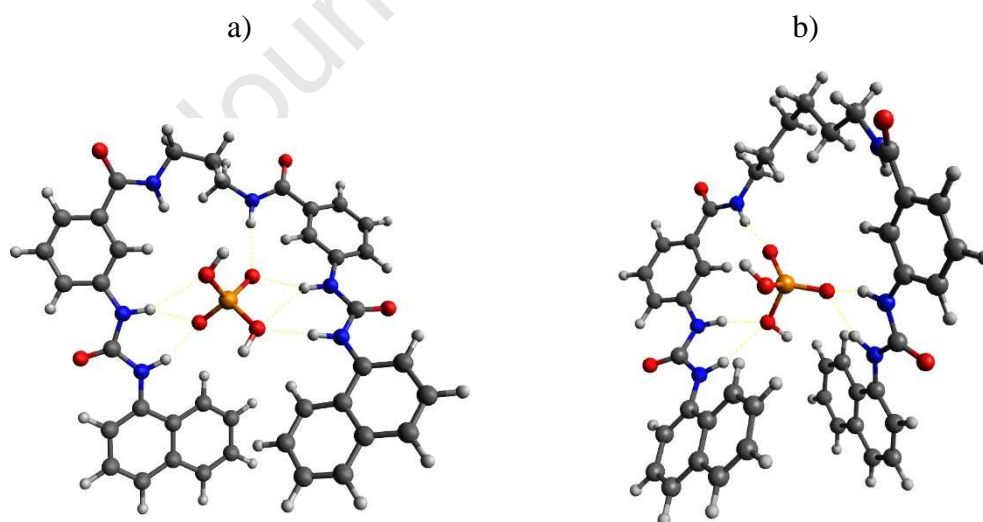


**Figure 15.** Optimized geometries of **m3N-HP** (a) and **m6N-HP** (b) complexes by DFT.

The signals of **m3N** and **m6N** show an interesting behavior in the titration with HPP. The absence of urea signals since the first aliquot added and the change of a colorless solution to an orange color indicate deprotonation by an acid-base reaction. However, the  $\text{H}_{e,e'}$  signal shifts 2.3 ppm to downfield when 1.2 equivalents of HPP are added due

to the interaction of this hydrogen with HPP (Figure 16). In addition, all the signals remain constant when more equivalents of HPP are added. This result demonstrates high affinity and the presence of a 1:1 complex in the solution. Similar results were obtained in the titration of **m6N** with HPP (Figure S25).

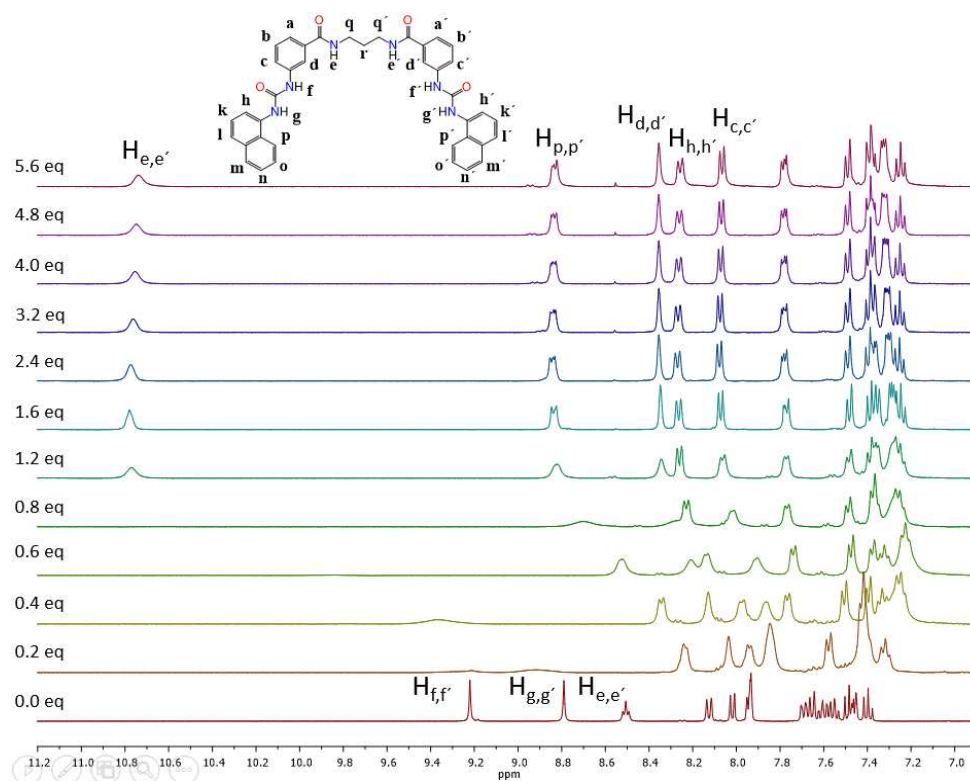


**Figure 16.** Partial  $^1\text{H}$  NMR spectra obtained in the titration of **m3N** [6 mM] with TBAHPP in  $\text{DMSO-}d_6$ .

The optimized geometries of **m3N-HPP** and **m6N-HPP** complexes show the interaction of both ureylbenzamide units with the HPP anion where  $\text{H}_{\text{e,e}'}$ ,  $\text{H}_{\text{f,f}'}$ ,  $\text{H}_{\text{g,g}'}$ ,  $\text{H}_{\text{d,d}'}$  and  $\text{H}_{\text{p,p}'}$  are oriented to the anion. The flexibility of the alkyl chain in **m3N** and **m6N** allows the conformational changes necessary to maintain the interaction with the anion despite their length (Figure 17).

a)

b)

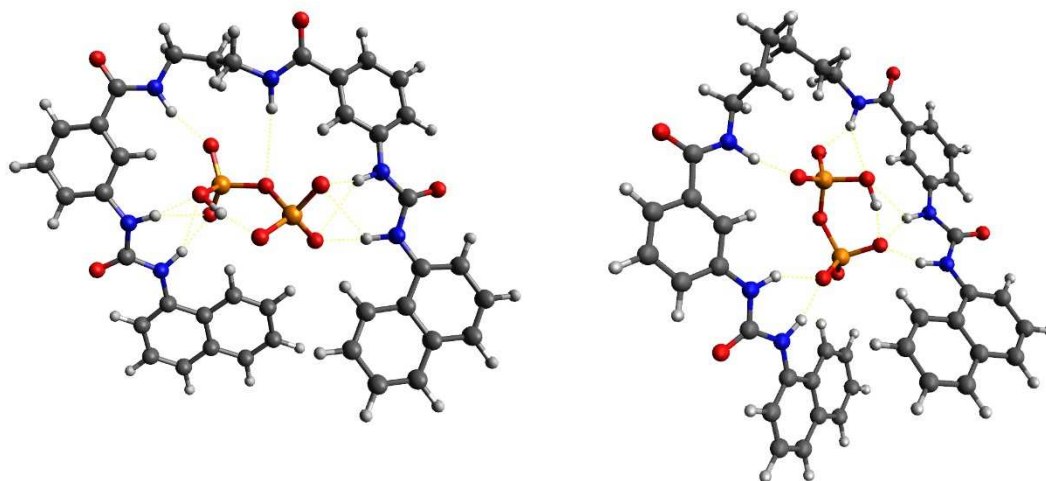


**Figure 17.** Optimized geometries of **m3N-HPP** (a) and **m6N-HPP** (b) complexes by DFT.

The urea ( $H_{f,f'}$  and  $H_{g,g'}$ ) and amide ( $H_{e,e'}$ ) signals of **o3N** and **o6N** show a slight shift to downfield in the titration with AcO and BzO, indicating the participation of both groups in the recognition process (Figures 18, S26-28). The chemical shift of the  $H_{e,e'}$  signal to downfield is more remarkable in **o3N** receptor (0.27 ppm) compared to **o6N** (0.05 ppm). As can be noted, the chemical shift of amide and urea signals in *ortho* receptors are smaller than in *meta* receptors, which may indicate a weaker anion-receptor interaction. The aromatic and naphthalic signals  $H_{a,a'}$ ,  $H_{p,p'}$ ,  $H_{k,k'}$ ,  $H_{m,m'}$  slightly shift to downfield and/or up-field, probably due to conformational changes.

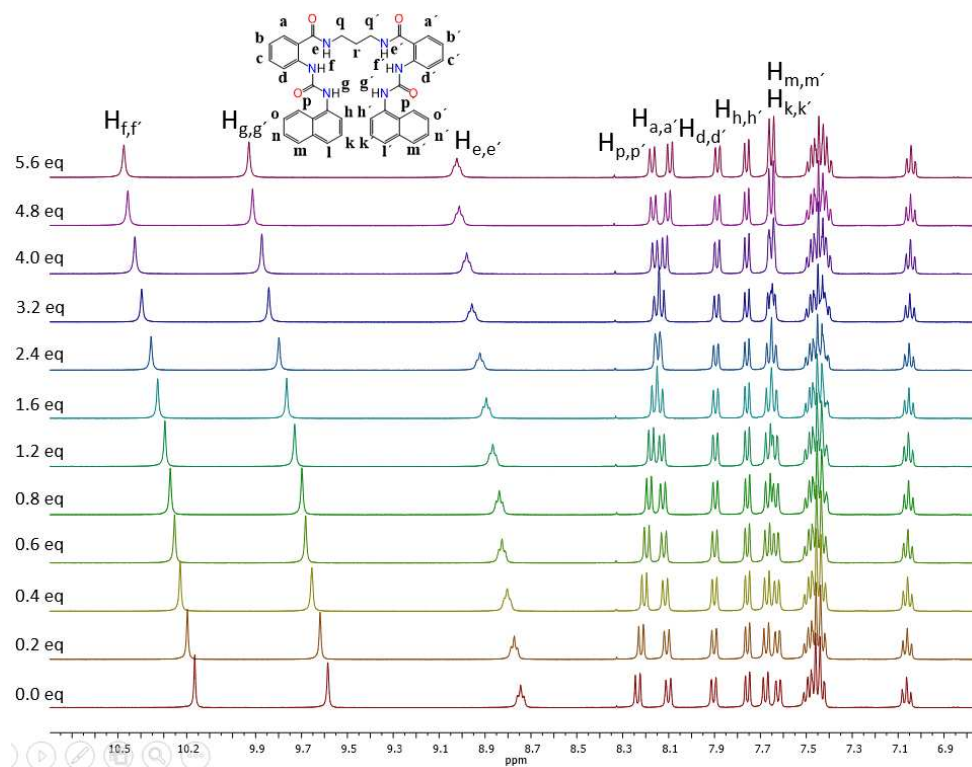


**Figure 18.** Partial  $^1\text{H}$  NMR spectra obtained in the titration of **o3N** [6 mM] with TBAAcO in  $\text{DMSO-}d_6$ .

The geometry of **o3N** and **o3N-AcO** and **o6N-AcO** complexes were optimized by DFT at the same theory level than *meta* complexes (Figure 19). The relative *ortho* position of urea and benzamide group induces the formation of an intramolecular hydrogen bond between the amide carbonyl and the  $\text{H}_{f,f'}$  hydrogen in **o3N** (Figure 19a). Also, there is not coplanarity between the naphthyl and urea-benzamide structure and the naphthyl groups adopt an *exo* position respect to the urea. Noteworthy, the receptors adopt a helical conformation in the complexes in order to minimize the distance with the carboxylate, and the helical conformation is less distorted as greater is the length of the alkyl chain. In fact, in **o6N-AcO** the ureylbenzamide units adopt an antiparallel position (Figure 19c). The naphthyl groups maintain the *exo* position due to the steric hindrance. As seen, the carboxylate binds to  $\text{H}_{f,f'}$ ,  $\text{H}_{g,g'}$  and  $\text{H}_{e,e'}$  with one ureylbenzamide unit and interacts with the other ureylbenzamide unit through the urea-hydrogens. These interactions are consistent with the changes observed in the hydrogen signals by  $^1\text{H}$ -NMR experiments.

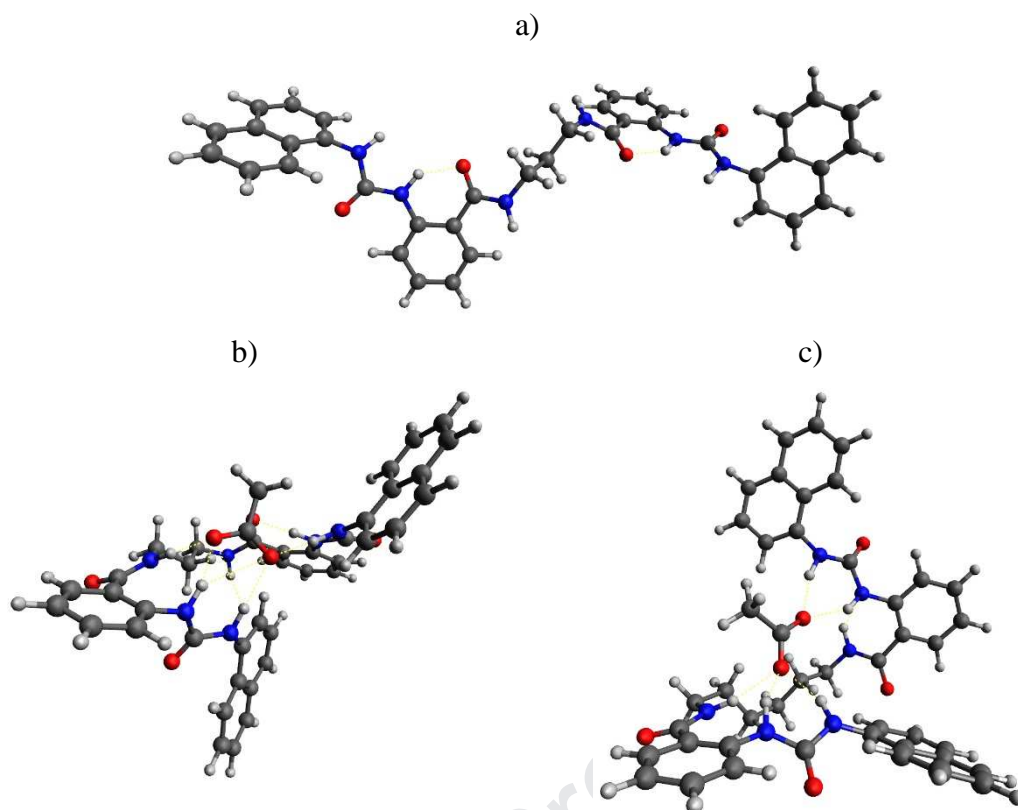


**Figure 19.** Optimized geometries of **o3N** (a), **o3N-AcO** (b) and **o6N-AcO** (c) by DFT.

A strong interaction with fluoride is evidenced by chemical shifts, widening and the absence of signals corresponding to the urea ( $H_{f,f'}$  and  $H_{g,g'}$ ) and amide groups ( $H_{e,e'}$ ) (Figure 20). The  $H_{f,f'}$  and  $H_{e,e'}$  signals shift downfield 0.78 ppm and 1.36 ppm, respectively, while  $H_{g,g'}$  signal shifts downfield and apparently disappears after one equivalent of the salt is added. However, the  $H_{g,g'}$  signal reappears overlapped with the  $H_{f,f'}$  signal at 10.95 ppm. The integration of this signal indicates that both hydrogens still present in the molecule (Figure S29). The signals corresponding to the naphthyl and phenyl ring are also affected following the same pattern observed in the titration with TBAAcO. The spectral changes in the titration of **o6N** are different than those observed with **o3N**, the urea and amide signals become broad during the course of the titration, then disappear when 4.0 equivalents of fluoride are added, and a triplet signal corresponding to  $[F-H-F]^-$  anion appears at 16.1 ppm, indicating an acid-base reaction at high concentration of F (Figures S30 and S31).

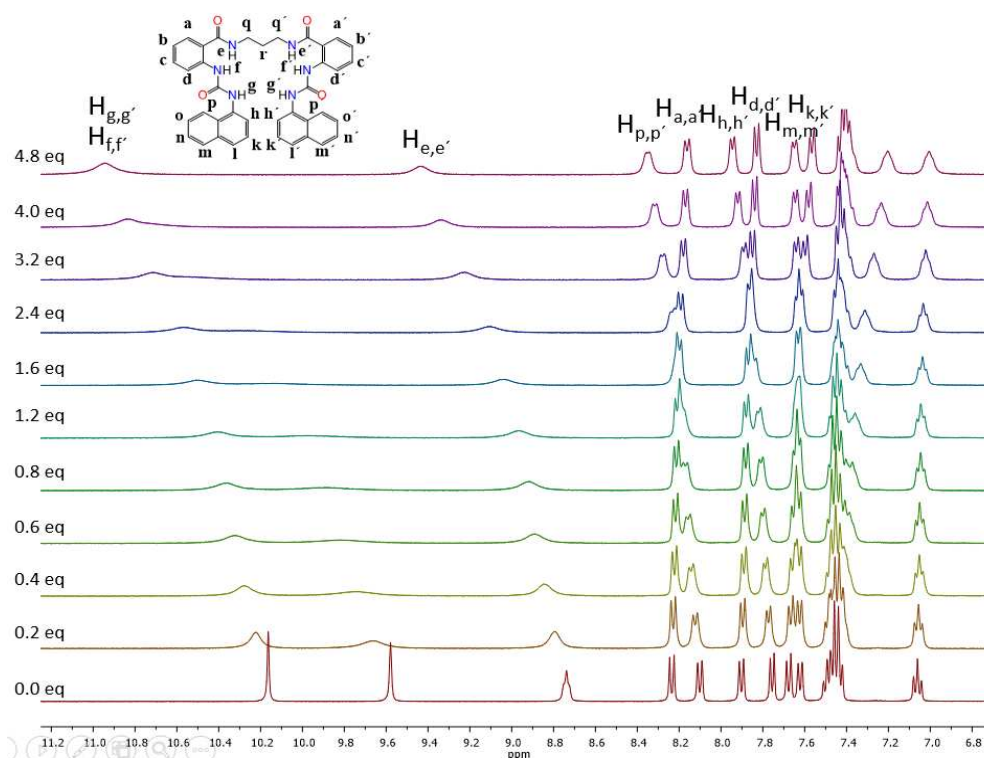


**Figure 20.** Partial  $^1\text{H}$  NMR spectra obtained in the titration of **o3N** [6 mM] with TBAF in  $\text{DMSO-}d_6$ .

The chemical shift difference in the  $\text{H}_{f,f'}$  and  $\text{H}_{g,g'}$  signals is visualized in the optimized geometry of **o3N-F** complex (Figure 21a). The distance of F and  $\text{H}_{g,g'}$  is shorter (1.66 Å average) compared with  $\text{H}_{f,f'}$  (1.94 Å average). Also, the interaction of F with one of the amide hydrogens is observed. The optimized geometry of **o6N-F** complex shows the interaction of F with both urea groups and the distance with  $\text{H}_{g,g'}$  is shorter (1.6 Å average) than  $\text{H}_{f,f'}$  (2.05 Å average). If amide hydrogens are too far from F (3.3 Å average), then the effect of fluoride over this hydrogen is minimal (Figure 21b).

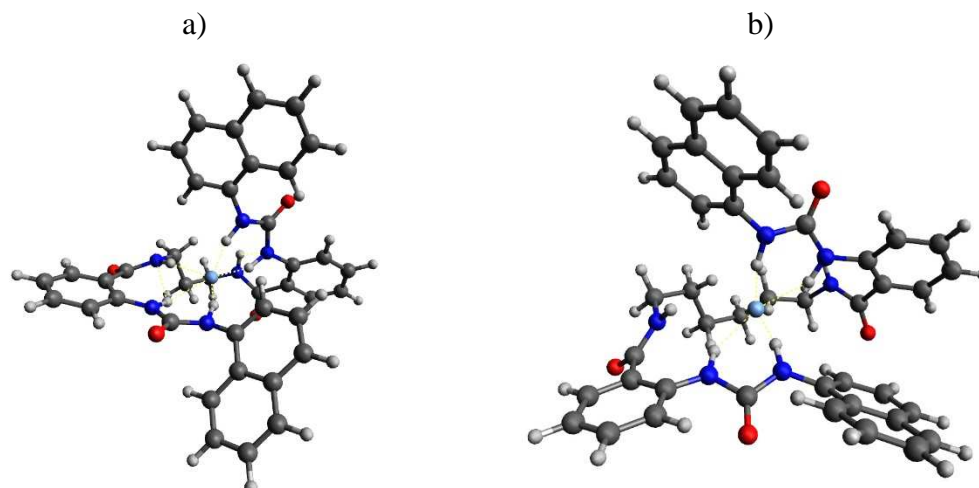


**Figure 21.** Optimized geometries of **o3N-F** (b) and **o6N-F** (c) by DFT.

The HP induces a downfield shift and broadening of  $H_{f,f'}$  (0.32 ppm),  $H_{g,g'}$  (0.43 ppm) and  $H_{e,e'}$  (0.71 ppm) signals, suggesting the interaction of amide and urea groups with the anion (Figure 22). Again, the effect over the urea hydrogens is not equal, due to a different interaction strength. The naphthyl and phenyl signals are also affected following a pattern previously described. Similar changes are observed in **o6N**, but the chemical shift of the signals involved are lower (Figure S32). The tetrahedral geometry of HP induces distortion of the helical conformation of receptors in the optimized geometry of **o3N-HP** and **o6N-HP** complexes in order to maximize their interaction (Figure 23). Multiple hydrogen bond interactions with the anion are established, and the distances with  $H_{f,f'}$  and  $H_{g,g'}$  are not equal, indicating a different interaction strength. Also, the hydrogen bonding distances are larger in **o6N-HP** complex due to a longer alkyl chain in this receptor. All these characteristics are consistent with the spectral changes observed in the  $^1\text{H}$  NMR spectra.

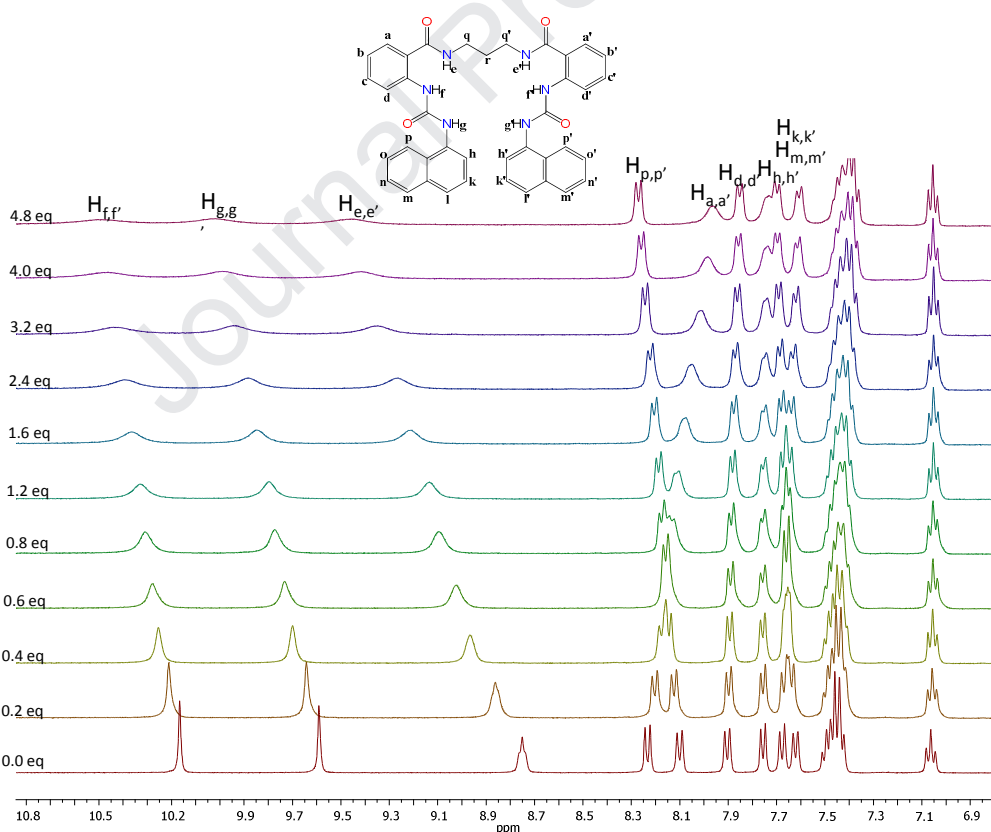


**Figure 22.** Partial  $^1\text{H}$  NMR spectra obtained in the titration of **o3N** [6 mM] with TBAHP in  $\text{DMSO-}d_6$

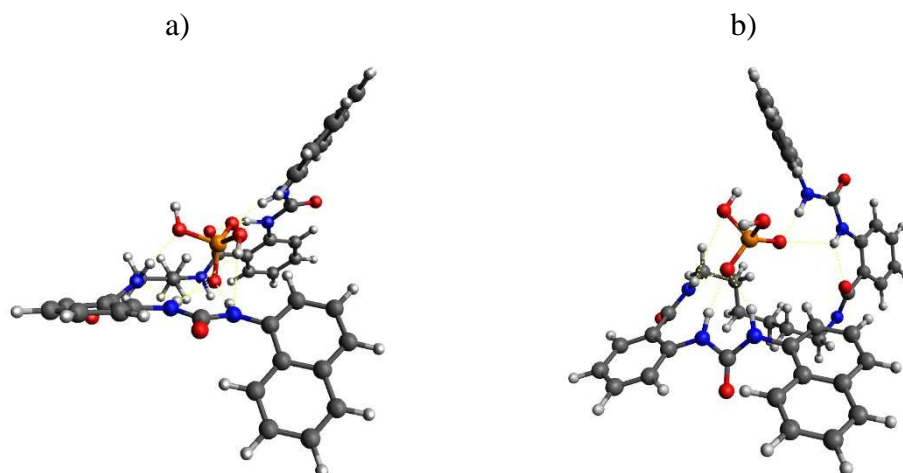


**Figure 23.** Optimized geometries of **o3N-HP** (a) and **o6N-HP** (b) by DFT.

The NMR spectra of **o3N** and **o6N** with HPP show broadening and downfield shift of  $H_{f,f'}$ ,  $H_{g,g'}$  and  $H_{e,e'}$  signals since the first aliquot added (0.2 equivalent). Then, there are an absence of  $H_{f,f'}$ ,  $H_{g,g'}$  and  $H_{e,e'}$  signals and change of colorless solution to an orange color indicating a deprotonation due to the high basicity of the HPP anion and the acidity of **o3N** (Figure 24 and S33). The optimized geometries of **o3N-HPP** and **o6N-HPP** shows multiple hydrogen bonding interactions between the receptor and the anion. The HPP accommodates in the way that it interacts with the two amide and the four urea hydrogens as it was observed in the NMR experiments (Figure 25).

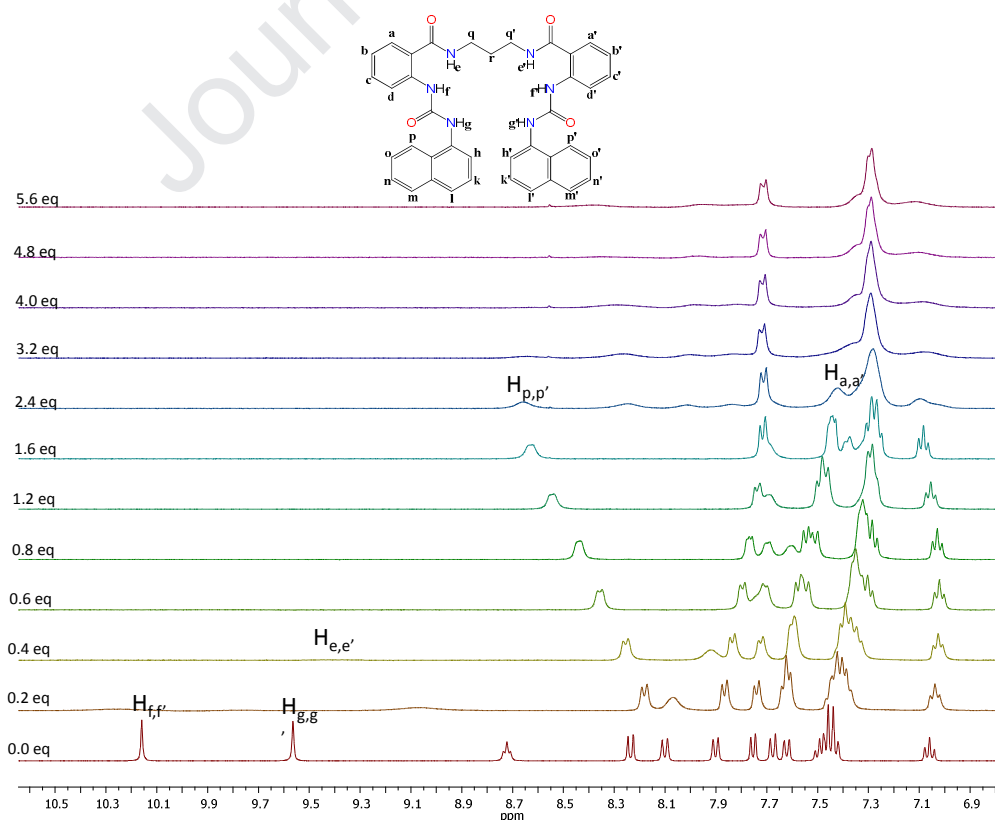


**Figure 24.** Partial  $^1\text{H}$  NMR spectra obtained in the titration of **o3N** [6 mM] with TBAHPP in  $\text{DMSO-}d_6$ .

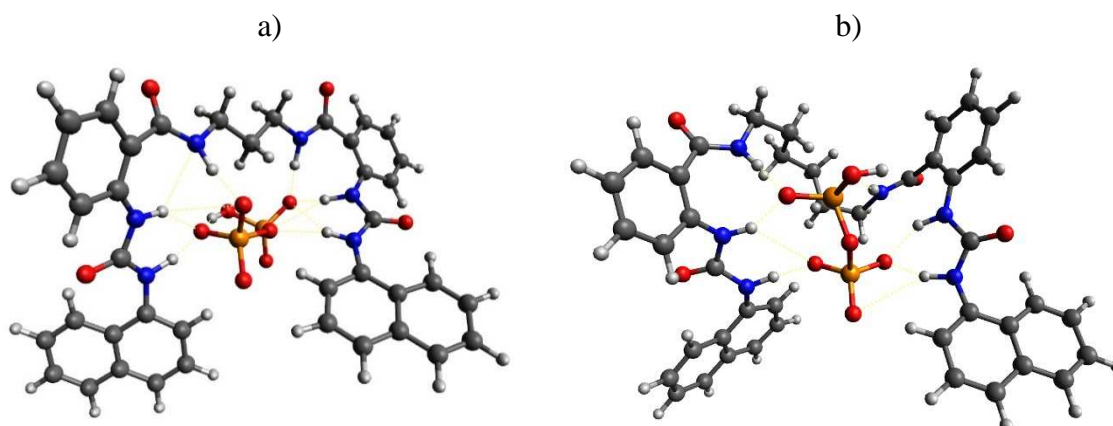


**Figure 25.** Optimized geometries of **o3N-HPP** (a) and **o6N-HPP** (b) complexes by DFT.

In general, the  $^1\text{H}$  NMR experiments show differences in the recognition process due to the relative position of urea and amide groups, the anions geometry and basicity. The participation of both amide and urea groups in the recognition process occur with fluoride and the tetrahedral anions HP and HPP in the **m3N** and **m6N** complexes. Therefore, the interaction of the trigonal AcO and BzO anions mainly occurs with the urea leaving out the amide group. In addition, in **o3N** and **o6N** participate both urea and amide groups during recognition of all the studied anions, due to the proximity of the functional groups.

The association constants ( $K$ ) were calculated from the data obtained from the  $^1\text{H}$  NMR experiments. A non-linear fit was used for a 1:1 interaction model, this method is based on the principle of Equation 3.

Eqn. (3)

$$\delta_{obs} = \delta_H + 0.5\Delta\delta_{\infty} \left\{ \frac{[H]_T + [G]_T + \frac{1}{K} - \sqrt{\left([H]_T + [G]_T + \frac{1}{K}\right)^2 - 4[H]_T * [G]_T}}{[H]_T} \right\}$$

where  $\delta_{obs}$  is the observed chemical shift,  $\delta_H$  is the chemical shift of the free receptor,  $\Delta\delta_{\infty}$  is the maximum chemical shift change induced by the presence of a given guest,  $[G]_T$  is the total concentration of the guest,  $[H]_T$  is the total concentration of the receptor, and  $K$  is the association constant. Also, more refined calculations using the

HypNMR program confirmed the  $K$  values for 1:1 complexes. Interestingly, a 1:3 complex for **m3N** and HP was identified probably due to interaction with several HP units and/or the auto-association of the HP. This result is consistent with the experimental observations previously described. Table 3 lists the association constants for the complex calculated from the chemical shift data.

**Table 3.** Association constants ( $K$ ) determined by  $^1\text{H}$  NMR for the anion-receptor interaction of **m3N**, **m6N**, **o3N** and **o6N**.

<b>TBAX</b>	<b>m3N</b> $K$ ( $\text{M}^{-1}$ )	<b>m6N</b> $K$ ( $\text{M}^{-1}$ )	<b>o3N</b> $K$ ( $\text{M}^{-1}$ )	<b>o6N</b> $K$ ( $\text{M}^{-1}$ )
<b>AcO</b>	44.0	24.6	85.2	75.3
<b>BzO</b>	110.0	60.3	37.8	102.3
<b>F</b>	87.0	190.8	25.6	<sup>a</sup> ND
<b>HP</b>	199.5 <sup>b</sup> $6.3 \times 10^5$	110.4	32.2	46.1
<b>HPP</b>	<sup>a</sup> ND	<sup>a</sup> ND	<sup>a</sup> ND	<sup>a</sup> ND

<sup>a</sup>ND: Not determined. An acid-based reaction was observed with the anion and/or according to the obtained data a non-linear adjustment was not achieved, and therefore the association constants could not be determined.

<sup>b</sup>  $K$  value for a 1:3 complex.

## Conclusions

Fluorescent bis(naphthylureylbenzamide)-based receptors are capable to interact with different anions. The supramolecular anion-receptor interaction is modulated by the structural characteristics of receptors such as the relative position of the urea and amide groups (*ortho* or *meta*), as well as, the geometry and charge of the anions. The urea hydrogens are more acid in *ortho* receptors and they are more susceptible to deprotonation in the presence of more basic anions as F and HPP. The **o(3-8)N** receptors exhibit greater steric hindrance compared with **m(3-8)N** receptors hindering interaction with anions. The *meta* receptors show great spectroscopic changes and they have a typical *ON/OFF* fluorescent response in the interaction with the anions, but an increase in fluorescence is observed with HPP in a 2:1 (receptor:anion) ratio. An *ON<sup>1</sup>/OFF/ON<sup>2</sup>* response is observed in the receptors with shorter alkyl spacer (**m3N** and **m4N**) with this anion. Noteworthy, the *ortho* receptors have an *OFF/ON* fluorescence response with all the studied anions, but the highest sensibility was obtained with HP and HPP and the receptors with shorter spacer **o3N** and **o4N**. The  $^1\text{H}$  NMR studies and

the theoretical analysis revealed significant differences in the site of interaction depending on the *ortho* and *meta* configuration, as well as, the size and geometry of the anions. Different *Log K* values, anion selectivity, and binding stoichiometry are observed depending on the technique utilized for the analysis. These differences are mainly attributed to the different concentration and solvent used in the experiments performed.

### Acknowledgements

Authors thank Consejo Nacional de Ciencia y Tecnología (CONACyT México) (Grant No. CB-2014-239581) and Tecnológico Nacional de México (Grant No. 5366.19-P) for the financial support for this project. Luis Miguel López-Martínez and José García-Elías thank CONACyT for the postdoctoral and graduate fellowship. The authors acknowledge grateful the support from Supramolecular Chemistry Thematic Network (CONACyT Grant No. 281251) and to the ITT NMR facilities (Grant INFR-201103-173395).

### References

1. Gale, P. A.; Caltagirone, C.; Anion sensing by small molecules and molecular ensembles. *Chem. Soc. Rev.* **2015**, *44*, 4212-4227.
2. Haridas, V.; Bijesh, M. B.; Dhawan, S.; Shandilya, A.; Peptide-triazole hybrid receptors for anion recognition. *Sens. Actuator B-Chem* **2017**, *245*, 903-910.
3. Emami Khansari, M.; Wallace, K. D.; Alamgir Hossain, M.; Synthesis and anion recognition studies of a dipodal thiourea-based sensor for anions. *Tetrahedron Lett.* **2014**, *55*, 438-440.
4. Moreno-Valle, B.; Aguilar-Martínez, M.; Ochoa-Terán, A.; Martínez-Quiroz, M.; Miranda-Soto, V.; García-Elías, J.; Ochoa-Lara, K.; Labastida-Galván, V.; Ordoñez, M.; Synthesis and anion recognition studies of new ureylbenzamide-based receptors. *Supramolecular Chem.* **2018**, *30*, 9-19.
5. Blazek, V.; Bregovic, N.; Mlinaric-Majerski, K.; Basaric, N.; Phosphate selective alkylenebisurea receptors: structure-binding relationship. *Tetrahedron* **2011**, *67*, 3846-3857.

6. Thale, P. B.; Borase, P. N.; Shankarling, G. S.; A “turn on” fluorescent and chromogenic chemosensor for fluoride anion: experimental and DFT studies. *Inorg. Chem. Front.* **2016**, *3*, 977-984.
7. Gale, P. A.; Structural and molecular recognition studies with acyclic anion receptors. *Acc. Chem. Res.* **2006**, *39*, 465-475.
8. Gale, P. A.; García-Garrido, S. E.; Garric, J.; Anion receptors based on organic frameworks: highlights from 2005 and 2006. *Chem. Soc Rev.* **2008**, *37*, 151-190.
9. Kaur, N.; Kaur, G.; Fegade, U. A.; Singh, A.; Sahoo, S. K.; Kuwar, A. S.; Singh, N.; Anion sensing with chemosensors having multiple eNH recognition units. *Trends Anal. Chem.* **2017**, *95*, 86-109.
10. Blackburn, A. L.; Baker, N. C. A.; Fletcher, N. C.; New insights into dihydrogenphosphate recognition with dirhenium(I) tricarbonyl complexes bridged by a thiourea moiety. *RSC Adv.* **2014**, *4*, 18442–18452.
11. Zwicker, V. E.; Yuen, K. K.; Smith, D. G.; Ho, J.; Qin, L.; Turner, P.; Jolliffe, K. A.; Deltamides and croconamides: expanding the range of dual H-bond donors for selective anion recognition. *Chem. Eur. J.* **2018**, *24*, 1140-1150.
12. Jennings, A. R.; Son, D. Y. Synthesis and anion recognition of three new preorganized colorimetric urea/thiourea compounds and their corresponding reference receptors. *Tetrahedron*, **2015**, *71*, 3990-3999.
13. Gale, P. A.; Caltagirone, C. Fluorescent and colorimetric sensors for anionic species. *Coord. Chem. Rev.* **2018**, *354*, 2-27.
14. Amendola, V.; Bergamaschi, G.; Boiocchi, M.; Fabbrizzi, L.; Mosca, L.; The interaction of fluoride with fluorogenic ureas: An  $ON^1-OFF-ON^2$  response. *J. Am. Chem. Soc.* **2013**, *135*, 6345-6355.
15. Santos-Figueroa, L. E.; Moragues, M. E.; Raposo, M. M. M.; Batista, R. M. F.; Costa, S. P. G.; Ferreira, R. C. M.; Sancenón, F.; Martínez-Máñez, R.; Ros-Lisa, J. V.; Soto, J.; Synthesis and evaluation of thiosemicarbazones functionalized with furyl moieties as new chemosensors for anion recognition. *Org. Biomol. Chem.* **2012**, *10*, 7418-7428.

16. Zhao, J.; Yang, D.; Yang, X.-J.; Wu, B.; Anion coordination chemistry: From recognition to supramolecular assembly. *Coord. Chem. Rev.* **2019**, *378*, 415-444.
17. Brooks, S. J.; Edwards, P. R.; Gale, P. A.; Light, M. E.; Carboxylate complexation by a family of easy-to-make orthophenylenediamine based bis-ureas: studies in solution and the solid state. *New J. Chem.* **2006**, *30*, 65-70.
18. Jin Cho, E.; Wha Moon, J.; Whan Ko, S.; Yong Lee, J.; Kyung Kim, S.; Yoon, J.; Chun Nam, K.; A new fluoride selective fluorescent as well as chromogenic chemosensor containing a naphthalene urea derivative. *J. Am. Chem. Soc.* **2003**, *125*, 12376-12377.
19. Blazek, V.; Mlinaric-Majerski, K.; Qin, W.; Basaric, N.; Photophysical study of the aggregation of naphthyl-, anthryl- and pyrenyl-adamantanebisurea derivatives. *J. Photochem. Photobiol A: Chem.* **2012**, *229*, 1-10.
20. Blazek, V.; Molcanov, K.; Mlinaric-Majerski, K.; Kojic-Prodic, B.; Basaric, N.; Adamantane bisurea derivatives: anion binding in the solution and in the solid state. *Tetrahedron* **2013**, *69*, 517-526.
21. Kondo, S.-I.; Nagamine, M.; Karasawa, S.; Ishihara, M.; Unno, M.; Yano, Y.; Anion recognition by 2,2'-binaphthalene derivatives bearing urea and thiourea groups at 8- and 8'-positions by UV-vis and fluorescence spectroscopies. *Tetrahedron* **2011**, *67*, 943-950.
22. Forbes, S., Hydrogen-bond driven supramolecular chemistry for modulating physical properties of pharmaceutical compounds. Department of Chemistry College of Arts and Sciences. *Kansas State University*, **2010**, 1-357.
23. Amendola, V.; Esteban-Gómez, D.; Fabbrizzi, L.; Licchelli, M.; What anions do to N-H-containing receptors. *Acc. Chem. Res.* **2006**, *39*, 343-353.
24. Amendola, V.; Boiocchi, M.; Esteban-Gómez, D.; Fabbrizzia, L.; Monzania, E.; Chiral receptors for phosphate ions. *Org. Biomol. Chem.* **2005**, *3*, 2632-2639.
25. Boiocchi, M.; Del Boca, L.; Esteban-Gómez, D.; Fabbrizzi, L.; Licchelli, M.; Monzani, E.; Anion-induced urea deprotonation. *Chem. Eur. J.* **2005**, *11*, 3097-3104.

26. Boiocchi, M.; Del Boca, L.; Esteban-Gómez, D.; Fabbrizzi, L.; Licchelli, M.; Monzani, E.; Nature of urea-fluoride interaction: incipient and definitive proton transfer. *J. Am. Chem. Soc.* **2004**, *126*, 16507-16514.
27. Jose, D. A.; Kumar, D. K.; Kar, P.; Verma, S.; Ghosh, A.; Ganguly, B.; Ghoshb, H. N.; Dasa, A.; Role of positional isomers on receptor-anion binding and evidence for resonance energy transfer. *Tetrahedron* **2007**, *63*, 12007-12014.
28. Russ, T. H.; Pramanik, A.; Khansari, M. E.; Wong, B. M.; Hossain, M. A.; A quinoline based bis-urea receptor for anions: a selective receptor for hydrogen sulfate. *Nat. Prod. Commun.* **2012**, *7*, 301-304
29. dos Santos, C. M. G.; McCabe, T.; Watson, G. W.; Kruger, P. E.; Gunnlaugsson, T. The recognition and sensing of anions through “positive allosteric effects” using simple urea-amide receptors. *J. Org. Chem.* **2008**, *73*, 9235-9244.
30. Hay, B. P.; Firman, T. K.; Moyer, B. A.; Structural design criteria for anion hosts: strategies for achieving anion shape recognition through the complementary placement of urea donor groups. *J. Am. Chem. Soc.* **2005**, *127*, 1810-1819.
31. Bryantsev, V. S.; Hay, B. P., De novo structure-based design of bisurea hosts for tetrahedral oxoanion guests. *J. Am. Chem. Soc.* **2006**, *128*, 2035-2042.
32. Frisch, M. J.; Trucks, G. W.; Schlegel, H. B.; Scuseria, G. E.; Robb, M. A.; Cheeseman, J. R.; Scalmani, G.; Barone, V.; Mennucci, B.; Petersson, G. A.; Nakatsuji, H.; Caricato, M.; Li, X.; Hratchian, H. P.; Izmaylov, A. F.; Bloino, J.; Zheng, G.; Sonnenberg, J. L.; Hada, M.; Ehara, M.; Toyota, K.; Fukuda, R.; Hasegawa, J.; Ishida, M.; Nakajima, T.; Honda, Y.; Kitao, O.; Nakai, H.; Vreven, T.; Montgomery, J. A.; Peralta, J. E.; Ogliaro, F.; Bearpark, M.; Heyd, J. J.; Brothers, K. N. Kudin, V. N. Staroverov, R. Kobayashi, J. Normand, K. Raghavachari, E.; Rendell, A.; Burant, J. C.; Iyengar, S. S.; Tomasi, J.; Cossi, M.; Rega, N.; Millam, J. M.; Klene, M.; Knox, J. E.; Cross, J. B.; Bakken, V.; Adamo, C.; Jaramillo, J.; Gomperts, R.; Stratmann, R. E.; Yazyev, O.; Austin, A. J.; Cammi, R.; Pomelli, C.; Ochterski, J. W.; Martin, R. L.; Morokuma, K.; Zakrzewski, V. G.; Voth, G. A.; Salvador, P.; Dannenberg, J. J.; Dapprich, S.; Daniels, A. D.; Farkas, O.; Foresman, J. B.; Ortiz, J. V.; Cioslowski, J.; Fox, D. J. Gaussian 09, Revision E.01. Gaussian, Inc., Wallingford CT, 2013.

33. Thordarson, P. Determining association constants from titration experiments in supramolecular chemistry. *Chem. Soc. Rev.* **2011**, *40*, 1305-1323.
34. Gans, P.; Sabatini, A.; Vacca, A.; Investigation of equilibria in solution. Determination of equilibrium constants with the HYPERQUAD suite of programs. *Talanta* **1996**, *43*, 1739-1753.
35. Gans, P.; Sabatini, A.; Vacca, A.; Determination of equilibrium constants from spectrophotometric data obtained from solutions of known pH: the program pHab. *Anal. Chim.* **1999**, *89*, 45-49.
36. Shokrollahi, A.; Zarghampour, F.; Akbari, S.; Salehi, A.; Solution scanometry, a new method for determination of acidity constants of indicators. *Anal. Methods* **2015**, *7*, 3551-3558.
37. Caltagirone, C.; Bazzicalupi, C.; Isaia, F.; Light, M. E.; Lippolis, V.; Montis, R.; Murgia, S.; Olivaria, M.; Picci, G.; A new family of bis-ureidic receptors for pyrophosphate optical sensing. *Org. Biomol. Chem.* **2013**, *11*, 2445-2451.
38. Landey-Álvarez, M. A.; Ochoa-Terán, A.; Pina-Luis, G.; Martínez-Quiroz, M.; Aguilar-Martínez, M.; Elías-García, J.; Miranda-Soto, V.; Ramírez, J.-Z.; Machi-Lara, L.; Labastida-Galván, V.; Ordoñez, M. Novel naphthalimide-aminobenzamide dyads as OFF/ON fluorescent supramolecular receptors in metal ion binding. *Supramolecular Chem.* **2016**, *28*, 892-906.
39. Gillen, D. M.; Hawes, C. S.; Gunnlaugsson, T. Solution-state anion recognition, and structural studies, of a series of electron-rich meta-phenylene bis(phenylurea) receptors and their self-assembled structures. *J. Org. Chem.* **2018**, *83*, 10398-10408.
40. Lakshminarayanan, P. S.; Ravikumar, I.; Suresh E.; Ghosh, P. Trapped inorganic phosphate dimer. *Chem. Commun.* **2007**, 5214–5216.
41. Blažek, V.; Molčanov, K.; Mlinarić-Majerski, K.; Kojić-Prodić, B.; Basarić, N. Adamantane bisurea derivatives: anion binding in the solution and in the solid state. *Tetrahedron* **2013**, *69*, 517-526.
42. Fatila, E. M.; Pink, M.; Twum, E. B.; Karty, J. A.; Flood, A. H. Phosphate–phosphate oligomerization drives higher order co-assemblies with stacks of cyanostar macrocycles. *Chem. Sci.* **2018**, *9*, 2863-2872.

43. Mungalpara, D.; Kelm, H.; Valkonen, A.; Rissanen, K.; Kellerd. S.; Kubik, S. Oxoanion binding to a cyclic pseudopeptide containing 1,4-disubstituted 1,2,3-triazole moieties. *Org. Biomol. Chem.* **2017**, *15*, 102-113.
44. He, Q.; Kelliher, M.; Bähring, S.; Lynch, V. M.; L. Sessler, J. L. A bis-calix[4]pyrrole enzyme mimic that constrains two oxoanions in close proximity. *J. Am. Chem. Soc.* **2017**, *139*, 7140–7143.
45. Barisic, D.; Cindro, N.; Jurabasic Kulcsár, M.; Tireli, M.; Uzarevic, K.; Bregovic, N.; Tomisic, V. Protonation and anion binding properties of aromatic bis-urea derivatives – apprehending the proton transfer. *Chem. Eur. J.* **2019**, *25*, 4695-4706.

### Highlights

- A library of new alkyl bis(naphthylureylbenzamide)-based receptors was prepared.
- The receptors with urea and amide groups in *meta* position display an  $ON^1/OFF/ON^2$  fluorescent response with dihydrogen phosphate and hydrogen pyrophosphate
- The *ortho* receptors display an  $OFF/ON$  fluorescent response with dihydrogen phosphate and hydrogen pyrophosphate.
- $^1\text{H}$  NMR experiments show different coordination modes depending on the relative position of urea and amide groups, spacer length and anion structure.
- Optimized geometries of receptor-anion complexes are presented

**Declaration of interests**

The authors declare that they have no known competing financial interests or personal relationships that could have appeared to influence the work reported in this paper.

The authors declare the following financial interests/personal relationships which may be considered as potential competing interests:

Journal Pre-proof